공학석사학위논문

연료전지 응용을 위한 항산화 기능을 갖는 그래핀 옥사이드가 도입된 폴리(아릴렌 에테르 술폰) 복합막의 합성과 분석

Synthesis and Characterization of Poly(arylene ether sulfone)/Functionalized Graphene Oxide Composite Membrane Having Antioxidant Property for Fuel Cell Applications

2016년 2월

서울대학교 대학원

화학생물공학부

배 중 문

Abstract

Synthesis and Characterization of Poly(arylene ether sulfone)/Functionalized Graphene Oxide Composite Membrane Having Antioxidant Property for Fuel Cell Applications

Jungmoon Bae

Polymer Chemistry

Department of Chemical & Biological Engineering

Seoul National University

Sulfonated poly(arylene ether sulfone) (SPAES) based composite membranes were prepared using hindered amine functionalized graphene oxide (HA-GO) as a hydroxyl radical scavenger to investigate the effect of functionalized GO filler on membrane properties such as chemical durability, mechanical properties, water absorption behavior, and proton conductivity. The SPAES was synthesized by nucleophilic addition, and the HA-GO was prepared by ring opening reaction between the amine unit in 4-Amino-2,2,6,6-tetramethylpiperidine and epoxy group in graphene oxide. When the HA-GO was incorporated into the SPAES

matrix, the mechanical strength, dimensional stability, and proton conductivity of the composite membranes were improved. Especially, the SPAES/HA-GO composite membranes revealed much enhanced chemical durability compared to the pristine SPAES membrane in Fenton's reagent at 70 ^{o}C due to antioxidant property of the hindered amine groups in HA-GO. Therefore, the SPAES/HA-GO composite membranes exhibited less destroyed surface structure, and lower proton conductivity decrease than the pristine SPAES membrane after immersing in Fenton's reagent at 90 ^{o}C.

Keywords: Hindered amine, Antioxidant, Sulfonated Poly(arylene ether sulfone) (SPAES), Graphene oxide (GO), Polymer electrolyte membrane fuel cell (PEMFC)

List of Tables

Table 1. Oxidative stability and mechanical properties of the membranes.

Table 2. IEC, water uptake, dimensional change of volume of the membranes, and proton conductivity at 90 ^{o}C, 50 % RH.

List of Figures

Figure 1. Synthesis of sulfonated poly(arylene ether sulfone) (SPAES).

Figure 2. ^{1}H-NMR spectra of SPAES.

Figure 3. Preparation of hindered amine graphene oxide (HA-GO).

Figure 4. FT-IR spectra of GO, HA-GO, and HA.

Figure 5. XPS spectra of HA-GO.

Figure 6. TGA curves of GO, and HA-GO under a N_2 atmosphere.

Figure 7. SEM images of the cross-section of the membranes. (a) SPAES, (b) SPAES/HA-GO_0.1, (c) SPAES/HA-GO_0.5, (d) SPAES/HA-GO_1.0, and (e) SPAES/HA-GO_3.0.

Figure 8. Oxidative stability of SPAES and SPAES/HA-GO composite membranes.

Figure 9. Proton conductivity of SPAES and SPAES/HA-GO composite membranes at 90 ^{o}C as a function of relative humidity.

Figure 10. Proton conductivity of SPAES, SPAES/HA-GO_0.5, and SPAES/GO_0.5 at 90 ^{o}C (a) before fenton test, and (b) after fenton test.

List of Contents

Abstract ---------- i

List of Tables----------iii

List of Figures----------iv

List of Contents----------vi

1. **Introduction**----------1

2. **Experimental**----------3

2.1. Materials----------3

2.2. Synthesis of sulfonated poly(arylene ether sulfone) (SPAES)----------4

2.3. Preparation of graphene oxide (GO) ----------5

2.4. Preparation of hindered amine grafted graphene oxide (HA-GO)----6

2.5. Preparation of composite membranes ----------7

2.6.Characterization----------7

3. Results and Discussion----------10

3.1. Synthesis of sulfonated poly(arylene ether sulfone) (SPAES)----------10

3.2. Characterization of functionalized graphene oxide----------15

3.3. Morphology of composite membranes----------21

3.4. Oxidative stability----------23

3.5. Mechanical properties----------27

3.6. IEC, water uptake, and dimensional change----------29

3.7. Proton conductivity----------32

4. Conclusion----------36

5. References----------37

6. Abstract in Korean----------42

1. Introduction

Subsequently to the industrial revolution, the conversion of chemical energy into electrical energy became more important due to the increase in the use of electricity. It leads to develop of variety technologies, and the polymer electrolyte membrane fuel cells (PEMFCs) is one of them.[1, 2] The PEMFCs are attractive as highly energy efficient and environmentally friendly alternative energy sources than other developing applications.[3, 4] The polymer electrolyte membrane (PEM), which is one of the most important components of PEMFCs, plays a vital role in conducting protons from the anode to the cathode and acts as a barrier. PEM should have a high proton conductivity, mechanical stability, and chemical stability for practical applications.[5]

The commercially available and most studied PEM materials are perfluorosulfonated ionomers, such as Nafion, due to their high proton conductivity value and good chemical stability.[6] But perfluorosulfonated ionomers have some limitations such as high cost, low operational temperature (< 80 ^{o}C), and high gas permeability. Therefore, many groups try to overcome these limitations by developing modified perfluorosulfonated ionomer derivatives and alternative materials such as aromatic hydrocarbon polymers. Several groups of

advanced aromatic hydrocarbon based polymers were synthesized to develop PEM materials such as sulfonated poly(arylene ether sulfone) (SPAES),[7-9] sulfonated poly(ether ether ketone) (SPEEK),[10, 11] sulfonated polyimide (SPI),[12] polybenzimidazole (PBI).[13-15] Those kind of aromatic hydrocarbon polymers have merits of low cost, high thermal stability, and low gas permeability. Among these alternatives, SPAES is a considerably attractive material because of its high stability under operation condition in fuel cell.[16]

Recently, durability of the PEM is one of the critical issues impending commercialization of PEMFCs.[17, 18] It has relevance to chemical degradation of membrane according to hydroxyl radicals. The chemical reaction on the catalyst in anode and cathode can produce hydroxyl radicals, which are widely known to be responsible for chemical attack on the membrane.[19, 20] In the sulfonated poly(arylene ether sulfone) case, two possible degradation mechanisms, detachment of the sulfonic groups and polymer chain scission, are believed.[21, 22] Detachment of the sulfonic groups in membrane will cause a lowering of proton conductivity and polymer chain scission will cause a cell lifetime issue. Several groups research membranes containing radical scavenger materials.[23-28] In addition, graphene oxide (GO) has been extensively used for polymer composites due to its large surface area, great mechanical strength, chemical stability, and functional groups. To enhance the physicochemical properties of GO

have recently been studied.[29-33]

In this study, hindered amine functionalized graphene oxide was prepared by ring opening reaction between graphene oxide and 4-Amino-2,2,6,6-tetramethylpiperidine for use as a filler to improve the chemical stability and mechanical strength of PEM. This study provides a description of the synthesis and properties of the composite membranes, including their oxidative stability, mechanical stability, water absorption properties, and proton conductivity.

2. Experimental

2.1.Materials

4,4’-Dihydroxybiphenyl (BP, 97.0%, Aldrich) was recrystallized from methanol. 4,4’-Dichlorodiphenylsulfone (DCDPS, 98.0%, Aldrich) was recrystallized from toluene and 3,3’-Disulfonate-4,4’-dichlorodiphenylsulfone (SDCDPS) was synthesized from DCDPS according to previous literature.[34] Graphite powders were received from BASF (Germany). 4-Amino-2,2,6,6-

tetramethylpiperidine (HA, 97.0%, TCI) was used as received. *N*-Methyl-2-pyrrolidone (NMP, 99.0%, Junsei) and *N*,*N*-Dimethylformamide (DMF, 99.5%, Junsei) were stored over molecular sieves. Potassium carbonate (K_2CO_3, 99.0%, Aldrich), Phosphorous pentoxide (P_2O_5, 99.99+%, Aldrich), Sodium nitrate ($NaNO_3$, 99.0%, Daejung), and Potassium permanganate ($KMnO_4$, 97.0%, Aldrich) were used as received. All other solvents and reagents were used as received from standard vendors.

2.2.Synthesis of sulfonated poly(arylene ether sulfone) (SPAES)

SPAES was synthesized by condensation reaction between the 4,4'-Dihydroxybiphenyl (BP) and the dichloro monomers such as 4,4'-Dichlorodiphenylsulfone (DCDPS), and 3,3'-Disulfonate-4,4'-dichlorodiphenylsulfone (SDCDPS). A 250 mL three-neck round bottom flask equipped with nitrogen inlet and outlet, Dean-Stark trap, condenser, and mechanical stirrer was charged with 5.00 g (26.9 mmol) of BP, 3.86 g (13.4 mmol)

of DCDPS, 6.60 g (13.4 mmol) of SDCDPS, and 4.27 g (30.9 mmol) of K_2CO_3 in 45.2 mL of NMP. Then 22.6 mL of toluene (NMP/toluene = 2/1, v/v) was added as an azeotroping agent. The mixture was heated 145 ^oC for 4 h. And the toluene was removed, the bath temperature was raised to 190 ^oC for polymerization. After 48 h, viscous solution was cooled down to room temperature and diluted with 10.0 mL of NMP. The solution was filtered and precipitated in *iso*-propylalcohol (1000mL) to remove the salt. And then, the white product obtained from precipitation was dried overnight under vacuum.

2.3.Preparation of graphene oxide (GO)

Graphene oxide (GO) was synthesized by the modified Hummer's method using graphite as starting materials. 1.0 g of graphite powder and 0.5 g of P_2O_5 were added to 6 mL of concentrated sulfuric acid (98.0%). The mixture was heated at 80 ^oC and stirred for 6 h. Next, 200 mL of deionized water was added to the mixture. Then the mixture was filtered and washed with deionized water several times. The obtained product (pre-oxidized graphite) was dried in vacuum

oven at 60 ^{o}C for 24 h. The dried pre-oxidized graphite and 0.5 g $NaNO_3$ were added to 23 mL of concentrated sulfuric acid (98.0%) in an ice bath for 30 min without stirring. Next, 6.0 g of $KMnO_4$ was added slowly with stirring. The mixture was heated to 35 ^{o}C and stirred for 18 h. Then 200 mL of deionized water and 10 mL of 30 % H_2O_2 were added. The mixture was washed rinsing and centrifugation with 10 wt.% of HCl and deionized water for several times. The obtained product (GO) was dried overnight at 60 ^{o}C.

2.4.Preparation of hindered amine grafted graphene oxide (HA-GO)

0.1 g of GO was added to 30 mL of anhydrous DMF and the mixture was sonicated for 30 min. 0.2 g of 4-Amino-2,2,6,6-tetramethylpiperidine (hindered amine compound, HA, 1.28 mmol) was added to the GO solution and the mixture was heated at 80 ^{o}C with stirring and purged under N_2 for 12 h. Purified HA-GO was obtained by filtering through PTFE membrane filter with 0.2 μm pore size and washing with DMF several times.

2.5.Preparation of composite membranes

Composite membranes were prepared by solution casting. 0.5 mg of HA-GO (HA-GO/SPAES = 0.1/1 wt./wt.) was added to 3.33 g of DMF. The solution was sonicated for 40 min, and stirred at 60 ^{o}C for 1 h to make a homogeneous dispersion. And then, 0.5 g of SPAES was added to the solution and stirred at 60 ^{o}C for 2 h. Next, the solution was spread onto a glass plate. Thickness of membrane was controlled by a doctor blade film applicator. The casted solution was heated at 80 ^{o}C for 12 h in a vacuum oven. The obtained film was peeled off from the glass plate with deionized water and soaked in H_2SO_4 for 24 h. And then, the film was washed with deionized water. The samples are assigned as SPAES/HA-GO_X, where X is the wt% of HA-GO (X = 0.1, 0.5, 1.0, 3.0). For comparison of the HA-GO and GO, SPAES/GO_X composite membranes were prepared by same method.

2.6.Characterization

The ^{1}H-NMR spectra was collected on Avance-400 (Bruker, Germany) with a proton frequency of 400 MHz. Deuterated dimethylsulfoxide (DMSO-d_6) and tetramethylsilane (TMS) were used as the solvent and the internal standard, respectively. M_n and M_w were measured by gel permeation chromatography (GPC) consisting of a Waters 510 HPLC pump at 35 ^{o}C, three columns PLgel 5 μm guard, MIXED-C, MIXED-D, and a Viscoter T60A dual detector. HPCL grade DMF was used as the eluent and the flow rate was 1.0 mL min^{-1}. Calibration was performed with polystyrene standards.

Fourier-transform infrared (FT-IR) spectra of samples were recorded on Nicolet 6700 (Thermo Scientific, USA) in the attenuated total reflectance (ATR) mode in the frequency range of 4000 to 650 cm^{-1}. The spectra were collected over 30 scans at 4 cm^{-1} resolution. Thermo gravimetric analysis (TGA) was performed in a Q-5000IR (TA instruments, USA). The samples were heated from 25 ^{o}C to 600 ^{o}C with a heating rate of 5 ^{o}C/min under nitrogen atmosphere. X-ray photoelectron spectroscopy (XPS) was carried out using MgKα (1254.0 eV) as the radiation source on a KRATOS AXIS-His. The spectra were collected over a range of 0-1200 eV. The cross-sectional morphology of the composite membranes was inspected by JSM-6700F (JEOL, Japan) using a field emission scanning electron microscope (FESEM).

The oxidative stability of the membranes was evaluated by Fenton's test. The membranes were soaked in Fenton's reagent (3% H_2O_2 containing 4 ppm Fe^{2+}) at 70^{o}C. The time when the membranes were degraded (τ_1) and dissolved (τ_2) was recorded. The mechanical properties were measured using a universal testing machine (UTM, Lloyd LR-10k, UK). And dumbbell specimens were prepared using the ASTM standard D638 (Type V specimens). The tensile properties of the samples were measured in air at 25 ^{o}C under a 40% relative humidity (RH) with a gauge length and cross head speed of 15 mm and 5 mm min^{-1}, respectively. At least 10 samples were tested for each sample.

Ion-exchange capacity (IEC) of the membranes was measured by back-titration method. The dry membranes were soaked in 1 M NaCl aqueous solution at 25 ^{o}C for 24 h. And the solution was titrated with 0.01 M NaOH aqueous solution. The value of IEC was calculated from the titration data as follows:

$$IEC\ [mequiv.g^{-1}] = (C_{NaOH} \cdot \triangle V_{NaOH} / W_s)\ X\ 1000$$

where C_{NaOH}, $\triangle V_{NaOH}$, and W_s are the concentration of NaOH (aq), the consumed volume of NaOH (aq), and the weight of the dry membrane, respectively. The water uptake and dimensional change of the membranes were determined by measuring their change in weight and volume. The dry membranes were cut into 1 cm X 5 cm, and then their weight and volumes were measured.

Thereafter, the membranes were put into deionized water at 30 ^{o}C and 90 ^{o}C for 24 h and 4 h, respectively. After the membranes were taken out and wiped, their weight and volumes were measured. The water uptake and dimensional change were calculated as follows:

Water uptake (%) = $[(W_{wet} - W_{dry})/W_{dry}] \times 100$

Dimensional change (%) = $[(V_{wey} - V_{dry})/V_{dry}] \times 100$

where W_{wet} and W_{dry} are the weight of the wet and dry membranes and V_{wet} and V_{dry} are the volume of the wet and dry membranes, respectively.

Proton conductivities of the composite membranes were measured using a conductivity measurement system (BekkTeck BT-552MX, USA) with a H_2 flow rate of 500 cm^3/min at 90^{o}C under different relative humidity (RH) conditions. The samples were pre-equilibrated at 90^{o}C and 70% RH for 2h, after that the conductivity of membrane was measured. The equilibrium RH was obtained after about 15 min of stabilization time.

3. Result and Discussion

3.1.Synthesis of sulfonated poly(arylene ether sulfone) (SPAES)

Sulfonated poly(arylene ether sulfone) was synthesized by nucleophilic addition between the 4,4'-Dihydroxybiphenyl (BP) and the dichloro monomers such as 4,4'-Dichlorodiphenylsulfone (DCDPS) and 3,3'-Disulfonate-4,4'-dichlorodiphenylsulfone (SDCDPS) in NMP which contained toluene as an azotropic agent (Fig. 1).[35] The chemical structure of SPAES was confirmed by ^{1}H-NMR spectroscopy (Fig. 2). Degree of sulfonation (DS) of polymer is important parameter affecting physical stability and proton conductivity of PEM. With increments of DS, the proton conductivity value of membrane increases because the membrane becomes more hydrophilic and absorbs more water, which facilitates proton transport. However, when the DS is above 50 %, the physical stability of membrane is not suitable for use fuel cell applications. Thus, we prepared SPAES with the DS of 50 % for the PEMFC test in our experiments. The DS of SPAES was calculated from the integral ratio of proton peaks in aromatic regions by following equation[36]

$$DS\ (\%) = [8 \cdot I_7 / (2 \cdot I_7 + I_{others})]\ X\ 100$$

where I_7 and I_{others} are the integral value of 7 proton signal and the sum of the integral value of other proton signals, respectively. According to Fig. 2, the DS of SPAES is 46 % although the feed molar ratio of SDCDPS and DCDPS is 1:1. Slightly different reactivity between SDCDPS and DCDPS is causing this

result.[35] The number average molecular weight (M_n) and weight average molecular weight (M_w) of the SPAES measured from the GPC were 36000 and 123000, respectively. We confirmed successful synthesis of SPAES with high molecular weight.

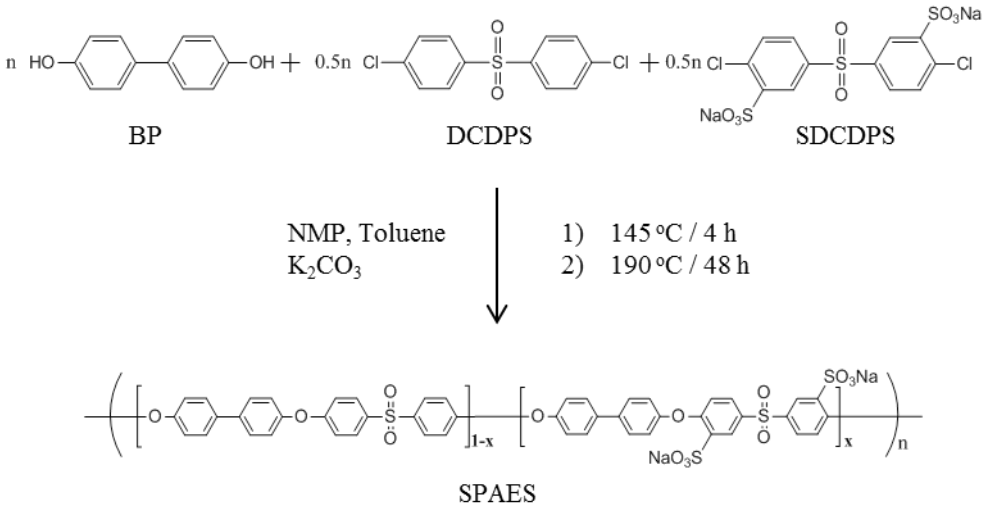

Figure 1. Synthesis of sulfonated poly(arylene ether sulfone) (SPAES).

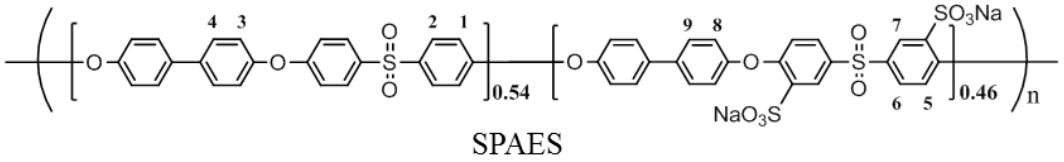

SPAES

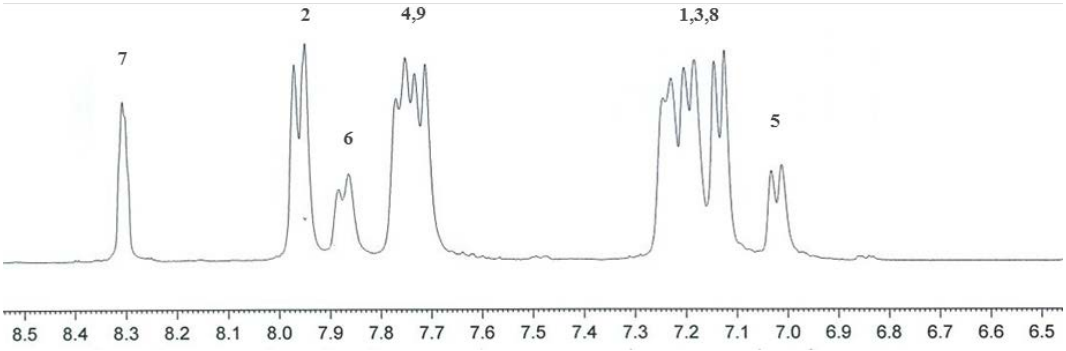

Figure 2. ^{1}H-NMR spectra of SPAES.

3.2.Characterization of functionalized graphene oxide

Graphene oxide (GO), and hindered amine functionalized graphene oxide (HA-GO) were prepared as shown in Fig. 3. GO was prepared from graphite by the modified Hummer's method with 6 weight equivalent amount of $KMnO_4$. HA-GO was prepared by ring opening reaction between the amine unit in hindered amine and epoxy group in GO. The chemical structure of GO and HA-GO was confirmed by FT-IR spectroscopy (Fig. 4). In the spectrum of GO, broad O-H stretching vibrations peak at 3450 cm^{-1}, C-O stretching vibrations peak at 1043 cm^{-1}, C=O stretching vibrations peak from carboxyl groups at 1740 cm^{-1}, and C-O-C stretching vibrations peak at 1248 cm^{-1} were observed.[37, 38] For HA-GO, peak of piperidine ring from the hindered amine at 2900-3000 cm^{-1}, and C-N stretching vibrations peak at 1440 cm^{-1} were observed. Also XPS results of HA-GO shown in the Fig. 5. The N 1_S peak was observed from the HA-GO.

The content of the grafted hindered amine on the GO were estimated by TGA (Fig. 6). The weight change below 300 °C of GO and HA-GO exhibits the thermal decomposition of the oxygen functional groups such as hydroxyl, epoxide, carboxylic acid, and ketone. And 14 wt% of the weight change of the HA-GO between 300 and 500 °C exhibits the thermal decomposition of the hindered

amine on the GO.[39] This results indicate the successful incorporation of the hindered amine unit into GO to from HA-GO.

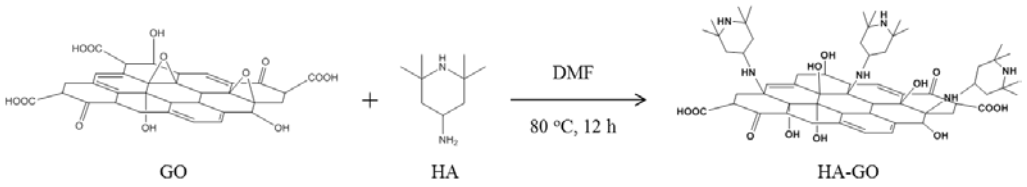

Figure 3. Preparation of hindered amine graphene oxide (HA-GO).

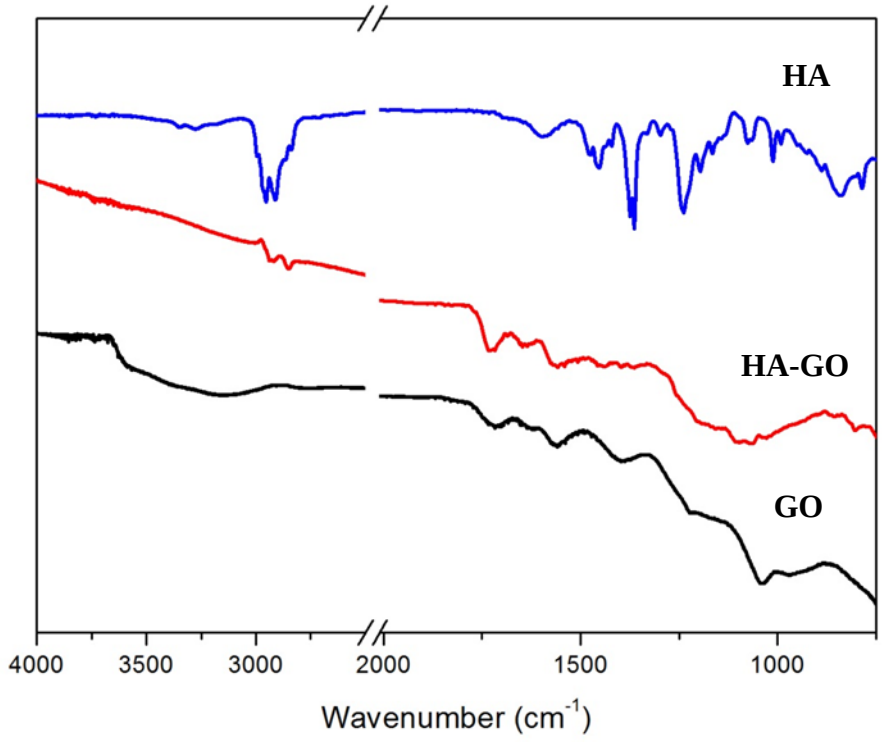

Figure 4. FT-IR spectra of GO, HA-GO, and HA.

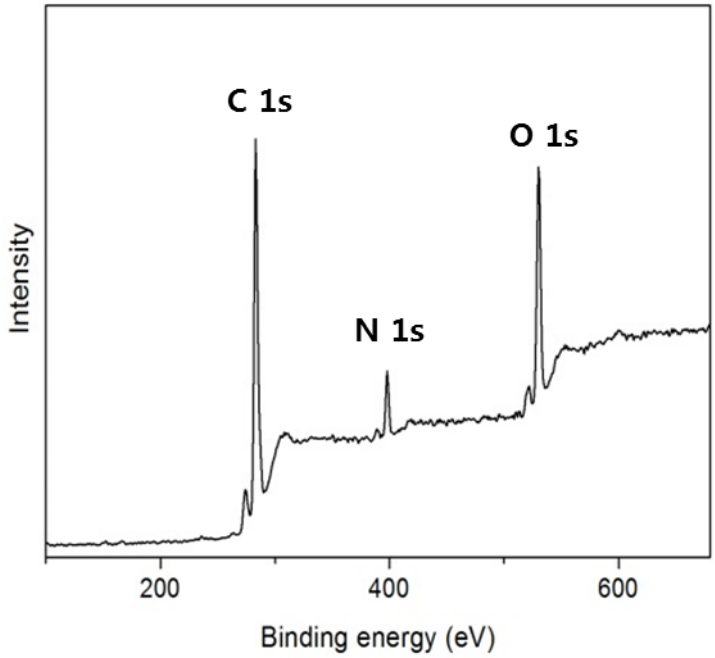

Figure 5. XPS spectra of HA-GO

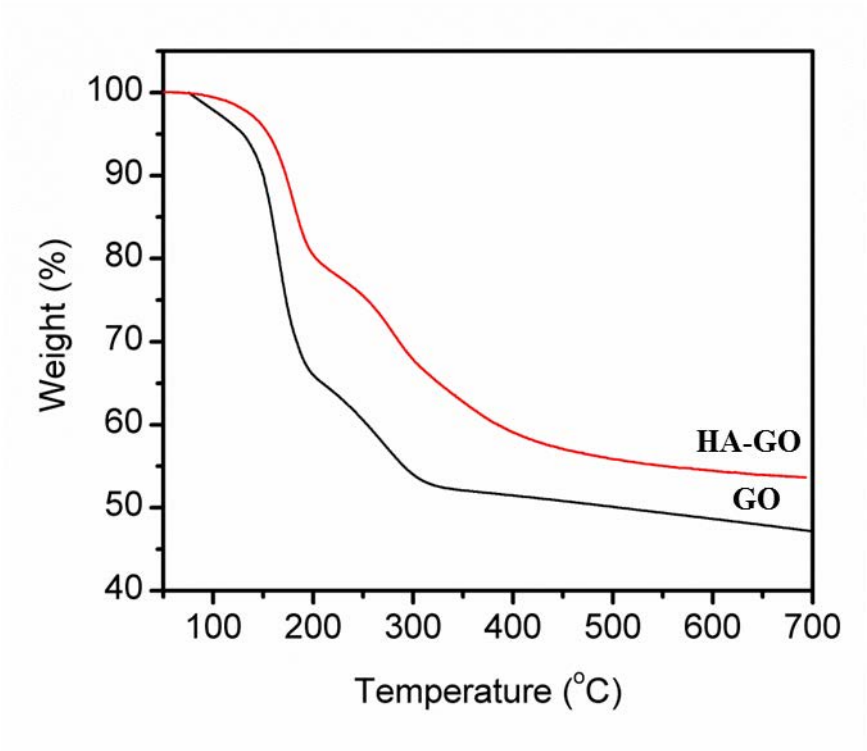

Figure 6. TGA curves of GO, and HA-GO under a N_2 atmosphere.

3.3.Morphology of composite membranes

The SPAES/HA-GO composite membranes were prepared successfully by solution casting method. Each thickness of the membranes was 15 ~ 20 μm. Internal morphology of the membranes showing filler dispersion was observed by cross-sectional SEM in Fig. 7. The cross-section of composite membranes was obtained by brittle breakage in liquid nitrogen. The pristine SPAES membrane showed relatively uniform and smooth cross-sectional features. But, when the HA-GO content increases, the morphology of the membranes became rougher due to the mutual interaction between the SPAES and HA-GO fillers. This result is because the GO generally has a poor dispersion in common organic solvent.[40] Especially, when HA-GO content is larger than 0.5 wt% in SPAES matrix, agglomerated domains form due to the poor dispersion of the HA-GO fillers. These agglomerated domains have a bad effect on drives of PEMFCs.[41]

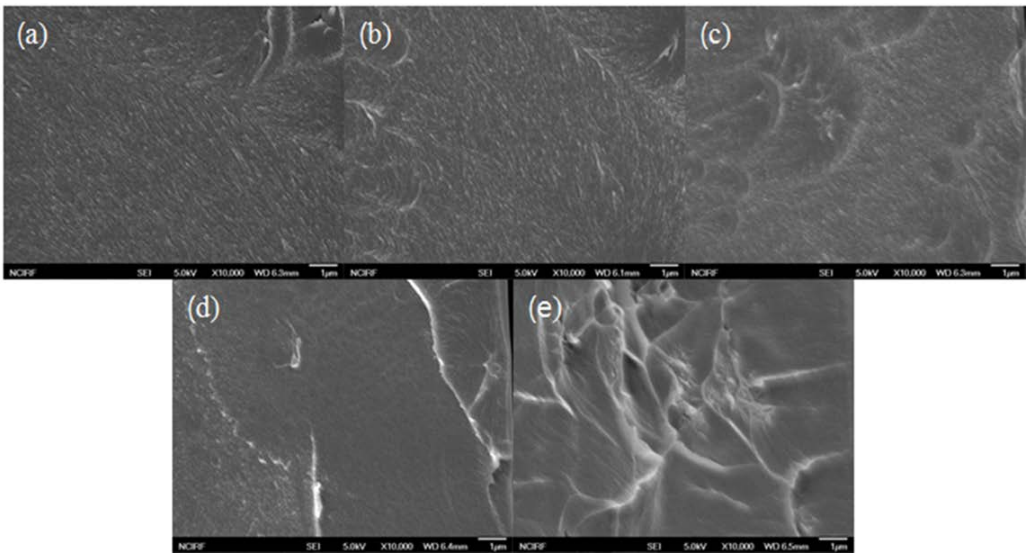

Figure 7. SEM images of the cross-section of the membranes. (a) SPAES, (b) SPAES/HA-GO_0.1, (c) SPAES/HA-GO_0.5, (d) SPAES/HA-GO_1.0, and (e) SPAES/HA-GO_3.0.

3.4.Oxidative stability

Oxidative stability is key parameter for durable PEM operation. The oxidative stability of SPAES/HA-GO composite membranes was investigated by Fenton test to evaluate the chemical stability of membranes against the attack of hydroxyl radical. The elapsed time was measured when the membranes start to break into pieces (τ_1), and the membranes are dissolved completely (τ_2) after immersion into Fenton's reagent (3 % H_2O_2 containing 4 ppm Fe^{2+}) at 70 ^oC. As shown in Fig. 8 and Table 1, the τ_1 and τ_2 value of the SPAES/HA-GO_0.5 were 480 min and 560 min, that of pristine SPAES were 387 min and 492 min, respectively. The oxidative stability increased by 24 % in τ_1 and 14 % in τ_2. It is observed that the incorporation of HA-GO into the SPAES matrix improved the oxidative stability of composite membranes compared to that of pristine SPAES when the content of the HA-GO contain below 0.5 wt% because HA works as a hydroxyl radical scavenger.[42] However, when the content of the HA-GO contain above 0.5 wt%, τ_1 and τ_2 value of composite membranes decreased. Because the aggregation of

HA-GO in the SPAES matrix when HA-GO contain above 0.5 wt% act the weak point that it is attacked by hydroxyl radicals.[43] Therefore, the addition of 0.5 wt% of HA-GO represents the most effective content to improve the oxidative stability of the PEM.

Table 1. Oxidative stability and mechanical properties of the membranes.

Samples	Fenton test		Tensile strength (MPa)	Elongation at break (%)
	τ_1 (min)	τ_2 (min)		
SPAES	387	492	62.9	10.3
SPAES/HA-GO_0.1	475	540	63.6	9.4
SPAES/HA-GO_0.5	480	560	65.3	6.5
SPAES/HA-GO_1.0	387	480	72.4	6.4
SPAES/HA-GO_3.0	340	450	73.4	6.2

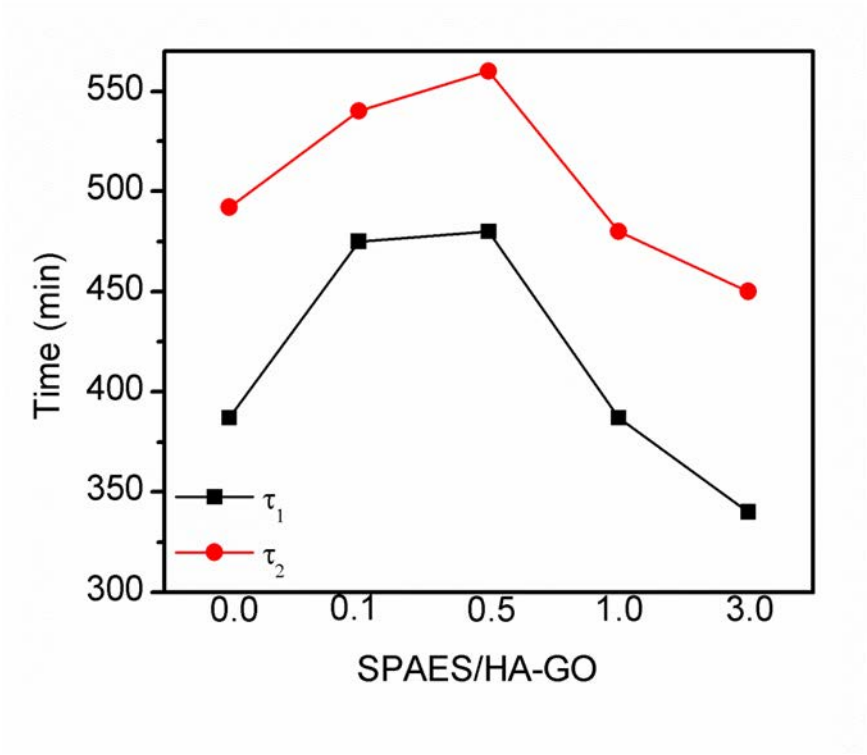

Figure 8. Oxidative stability of SPAES and SPAES/HA-GO composite membranes.

3.5.Mechanical properties

Adequate mechanical properties are essential for PEM for the fabrication of the membrane electrode assembly (MEA). The mechanical properties of membranes, such as tensile strength and elongation at break were measured by UTM under room temperature and 45 % RH conditions and shown in Table 1. The tensile strength of SPAES/HA-GO composite membranes was larger than pristine SPAES membrane and increased with increasing HA-GO content. On the contrary, elongation at break of SPAES/HA-GO composite membranes was smaller than pristine SPAES membrane and decreased with increasing HA-GO content. The SPAES/HA-GO_3.0 membrane had tensile strength of 74 MPa, and elongation at break of 6.1 %, that of pristine SPAES had tensile strength of 66 MPa, and elongation at break of 10.2 %. The tensile strength increased by 12 % and the elongation at break decreased by 40 % with the addition of HA-GO. Generally, the corporation of fillers, such as graphene and graphene oxide, in a polymer matrix enhances the mechanical strength by the reinforcement effect of the fillers.[44-46] Obviously, composite membranes increase the tensile strength and

decrease the elongation at break because HA-GO work as an effective filler in this study. This result demonstrated that the HA-GO as a filler in the polymer matrix was an effective approach for PEM with good mechanical properties.

3.6.IEC, water uptake, and dimensional change

IEC (the amount of exchangeable protons in membrane), water uptake, and dimensional change are important parameter affecting the quality of the PEM. In generally, PEM is required to have higher IEC and water uptake, but lower dimensional change, which would improve the performance of PEMFCs. The value of each parameter is shown Table 2. The IEC measured by a titration method. The IEC values decrease from 1.87 mequiv g^{-1} to 1.75 mequiv. g^{-1} when HA-GO contents increased.

The water uptake and dimensional change are the important factors which affect proton conductivity and mechanical properties of PEM. A suitable amount of water in membrane can forward proton transport, but excessive water absorption lead to side effects such as deterioration of mechanical strength.[41] Therefore, suitable water absorption is required for the PEMFCs. In this study, while functionalized graphene oxide formed free volume in polymer matrix to absorb water, strong interaction between functionalized graphene oxide and SPAES enhanced maintained dimensions. As expected, the water uptake increased with increasing the HA-GO content. The water uptake of SPAES/HA-GO_3.0 was 79.2 % at 30 ^{o}C and 121.5 % at 90 ^{o}C, and the water uptake of pristine SPAES

was 67.7 % at 30 ^{o}C and 93.1 % at 90 ^{o}C. The water uptake increased with increasing HA-GO content due to the hydrophilic nature of GO, and increasing free volume of polymer matrix.[43] The dimensional change of composite membranes decreased with increasing the HA-GO content. The dimensional change of SPAES/HA-GO_3.0 was 21.5 % at 30 ^{o}C and 29.9 % at 90 ^{o}C, and the dimensional change of pristine SPAES was 69.2 % at 30 ^{o}C and 101.3 % at 90 ^{o}C. The SPAES /HA-GO composite membranes exhibited smaller dimensional change value than pristine SPAES membrane due to the acid-base interaction between the amine groups of HA-GO and sulfonic acid groups of the SPAES.[41] The large water uptake and smaller dimensional change values of SPAES/HA-GO composite membranes can be beneficial for PEMFCs because it can increase proton conductivity and mechanical stability.

Table 2. IEC, water uptake, dimensional change of volume of the membranes, and proton conductivity at 90 ^{o}C, 50 % RH.

Samples	IEC (mequiv g^{-1})	Water uptake (%)		Dimensional change of volume (%)		Proton conductivity (mS cm^{-1})
		30 °C	90 °C	30 °C	90 °C	
SPAES	1.87	67.7	93.1	69.2	101.3	9.7
SPAES/HA-GO_0.1	1.83	71.3	106.6	33.9	64.3	12.1
SPAES/HA-GO_0.5	1.81	75.9	111.3	33.1	56.7	17.0
SPAES/HA-GO_1.0	1.77	78.4	119.6	28.3	45.2	15.0
SPAES/HA-GO_3.0	1.75	79.2	121.5	21.5	29.9	15.0

3.7.Proton conductivity

The proton conductivity is critical property of the PEM, since high proton conductivity is necessary for their effective utilization in PEMFCs. Fig. 9 and Table 2 show the humidity dependence of the proton conductivity for all membranes at 90 ^{o}C. The proton conductivity of SPAES and composite membranes is sensitive to humidity and rises with the increase in relative humidity (RH) from 20 to 100 %. And up to 0.5 wt% of HA-GO, the proton conductivity increased, but beyond 0.5 wt%, the proton conductivity decreased. The proton conductivity of SPAES/HA-GO_0.5 was 1.70 x 10^{-2} S cm^{-1}, that of pristine SPAES was 0.97 x 10^{-2} S cm^{-1} at 50 %RH. It increased by 75 % with the addition of HA-GO. This result is because the increase in hydrophilic moieties from the HA-GO which results in more hydrophilic channels in which protons can pass through. However, beyond 0.5 wt% of HA-GO show a reduction in proton conductivity values because aggregated HA-GO works as a barrier that disconnects the hydrophilic channels.

In addition, after fenton test (3% H_2O_2 containing 4 ppm Fe^{2+}) at 90 ^{o}C for 1 h, proton conductivity of membranes was measured for chemical durability of PEM at 90 ^{o}C. As shown in Fig. 10, the pristine SPAES membrane, the SPAES/HA-GO_0.5 exhibited best performance such as oxidative stability and proton

conductivity, and SPAES/GO_0.5 as control group were measured. Before fenton test, proton conductivity of the pristine SPAES, SPAES/HA-GO_0.5, SPAES/GO_0.5 were 0.97 x 10^{-2} S cm^{-1}, 1.70 x 10^{-2} S cm^{-1}, and 1.71 x 10^{-2} S cm^{-1}, respectively. Recent studies were reported that the proton conductivity of PEM increased when the GO was incorporated into polymer matrix.[47-49] The SPAES/GO_0.5 exhibited higher proton conductivity value than pristine SPAES membrane due to the increase in hydrophilic moieties from the GO. After fenton test, proton conductivity of the pristine SPAES, SPAES/HA-GO_0.5, and SPAES/GO_0.5 were 0.58 x 10^{-2} S cm^{-1}, 1.30 x 10^{-2} S cm^{-1}, and 1.16 x 10^{-2} S cm^{-1}, respectively. And decrease of the proton conductivity of the membranes was 40.2 %, 23.5%, and 32.2 %, respectively. Decrease of the proton conductivity of the SPAES/GO_0.5 is smaller than pristine SPAES because GO has antioxidant property. The SPAES/HA-GO_0.5 was exhibited the best performance in this test. This result is because the HA molecules on the GO would rapidly trap the hydroxyl radicals and stop their attacks to the polymer chain, thus giving much higher proton conductivity than pristine SPAES.[42]

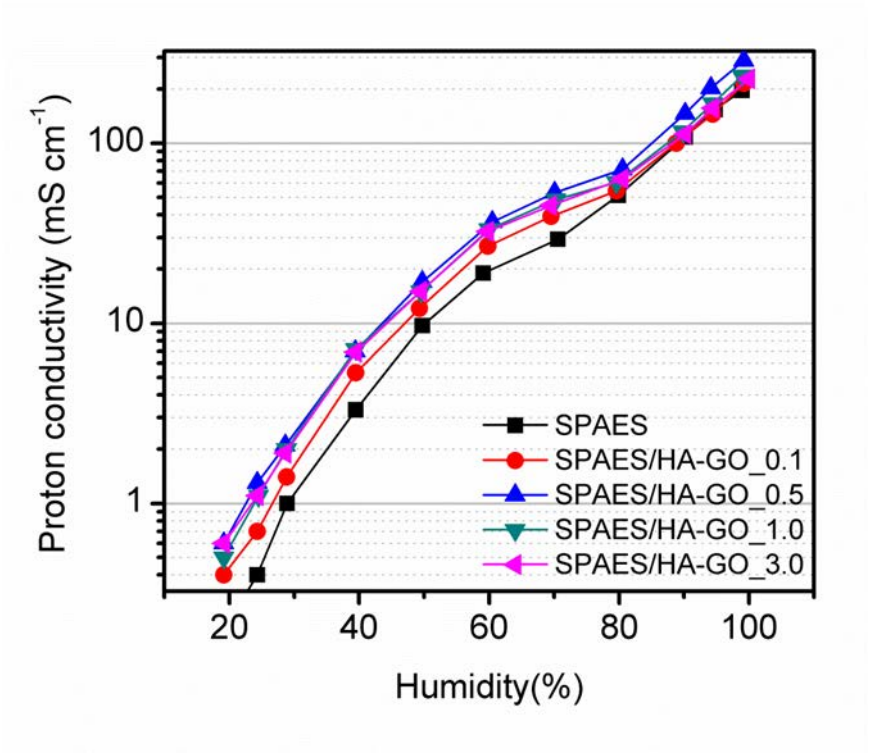

Figure 9. Proton conductivity of SPAES and SPAES/HA-GO composite membranes at 90 ^{o}C as a function of relative humidity.

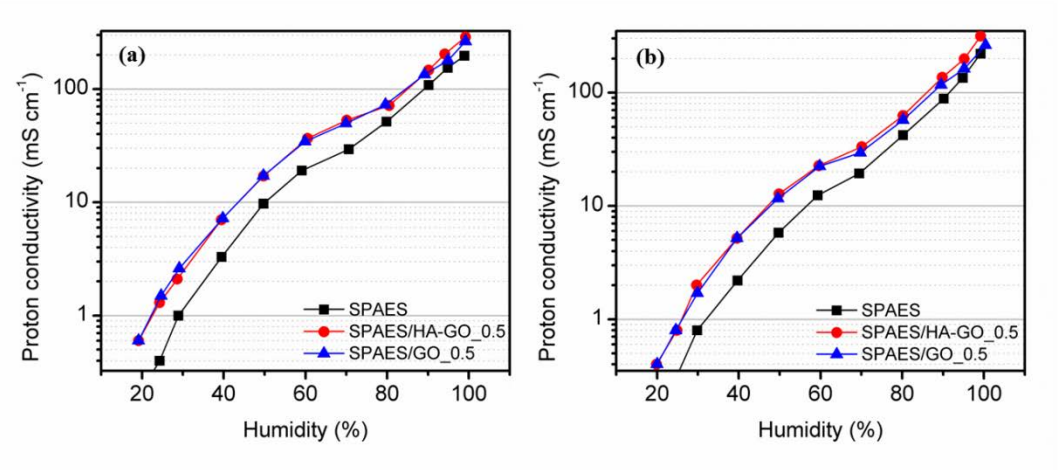

Figure 10. Proton conductivity of SPAES, SPAES/HA-GO_0.5, and SPAES/GO_0.5 at 90 ^{o}C (a) before fenton test, and (b) after fenton test.

4. Conclusion

Sulfonated poly(arylene ether sulfone) (SPAES) composite membranes were prepared using hindered amine (HA) grafted graphene oxide (HA-GO) for efficient polymer electrolyte membranes fuel cells (PEMFCs). The composite membranes showed improved mechanical properties and dimensional change due to an effective filler of HA-GO and acid-base interaction between SPAES and HA-GO. Especially, antioxidant property of the hindered amine should increase the oxidative stability of the membrane. SPAES/HA-GO_0.5 has shown better proton conductivity in comparison to pristine SPAES. Also, after fenton test at 90 ^{o}C for 1 h, decrease of the proton conductivity of the SPAES/HA-GO_0.5 was smaller than other membranes because HA-GO has antioxidant property. Therefore, we believe that the incorporation of HA-GO as a filler can be promising to develop proton exchange membranes for fuel cell applications.

5. References

1. Steele, B.C. and A. Heinzel, *Materials for fuel-cell technologies.* Nature, 2001. **414**(6861): p. 345-352.
2. Carrette, L., K. Friedrich, and U. Stimming, *Fuel cells–fundamentals and applications.* Fuel cells, 2001. **1**(1): p. 5-39.
3. Shao, Y., et al., *Proton exchange membrane fuel cell from low temperature to high temperature: material challenges.* Journal of Power Sources, 2007. **167**(2): p. 235-242.
4. Kim, S.-K., et al., *Durable cross-linked copolymer membranes based on poly (benzoxazine) and poly (2, 5-benzimidazole) for use in fuel cells at elevated temperatures.* Journal of Materials Chemistry, 2012. **22**(15): p. 7194-7205.
5. Hickner, M.A., et al., *Alternative polymer systems for proton exchange membranes (PEMs).* Chemical reviews, 2004. **104**(10): p. 4587-4612.
6. Paik, Y., S.S. Kim, and O.H. Han, *Methanol behavior in direct methanol fuel cells.* Angewandte Chemie International Edition, 2008. **47**(1): p. 94-96.
7. Kim, K., et al., *Semi-interpenetrating network electrolyte membranes based on sulfonated poly (arylene ether sulfone) for fuel cells at high temperature and low humidity conditions.* Electrochemistry Communications, 2014. **48**: p. 44-48.
8. Ko, T., et al., *Cross-Linked Sulfonated Poly (arylene ether sulfone) Membranes Formed by in Situ Casting and Click Reaction for Applications in Fuel Cells.* Macromolecules, 2015. **48**(4): p. 1104-1114.
9. Li, N., et al., *Enhancement of proton transport by nanochannels in comb-shaped copoly (arylene ether sulfone) s.* Angewandte Chemie, 2011. **123**(39): p. 9324-9327.
10. Xing, P., et al., *Synthesis and characterization of sulfonated poly (ether ether ketone) for proton exchange membranes.* Journal of Membrane Science, 2004. **229**(1): p. 95-106.
11. Zhao, C., et al., *High-performance proton exchange membranes for direct methanol fuel cells based on a SPEEK/polybenzoxazine crosslinked structure.* RSC Advances, 2015. **5**(59): p. 47284-47293.
12. Woo, Y., et al., *Synthesis and characterization of sulfonated polyimide*

membranes for direct methanol fuel cell. Journal of Membrane Science, 2003. **220**(1): p. 31-45.

13. Kim, S.-K., et al., *Highly durable polymer electrolyte membranes at elevated temperature: Cross-linked copolymer structure consisting of poly (benzoxazine) and poly (benzimidazole).* Journal of Power Sources, 2013. **226**: p. 346-353.
14. Kim, T.-H., T.-W. Lim, and J.-C. Lee, *High-temperature fuel cell membranes based on mechanically stable para-ordered polybenzimidazole prepared by direct casting.* Journal of Power Sources, 2007. **172**(1): p. 172-179.
15. Kim, S.-K., et al., *Cross-linked benzoxazine–benzimidazole copolymer electrolyte membranes for fuel cells at elevated temperature.* Macromolecules, 2012. **45**(3): p. 1438-1446.
16. Wang, F., et al., *Direct polymerization of sulfonated poly (arylene ether sulfone) random (statistical) copolymers: candidates for new proton exchange membranes.* Journal of Membrane Science, 2002. **197**(1): p. 231-242.
17. Zhao, D., et al., *A Durable Alternative for Proton-Exchange Membranes: Sulfonated Poly (Benzoxazole Thioether Sulfone) s.* Advanced Energy Materials, 2011. **1**(2): p. 203-211.
18. Alsheheri, J.M., H. Ghassemi, and D.A. Schiraldi, *Chemical degradation of fluorosulfonamide fuel cell membrane polymer model compounds.* Journal of Power Sources, 2014. **267**: p. 316-322.
19. Wu, J., et al., *A review of PEM fuel cell durability: degradation mechanisms and mitigation strategies.* Journal of Power Sources, 2008. **184**(1): p. 104-119.
20. Rodgers, M.P., et al., *Fuel cell perfluorinated sulfonic acid membrane degradation correlating accelerated stress testing and lifetime.* Chemical reviews, 2012. **112**(11): p. 6075-6103.
21. Lawrence, J. and T. Yamaguchi, *The degradation mechanism of sulfonated poly (arylene ether sulfone) s in an oxidative environment.* Journal of Membrane Science, 2008. **325**(2): p. 633-640.
22. Lawrence, J., K. Yamashita, and T. Yamaguchi, *Correlating electronic structure and chemical durability of sulfonated poly (arylene ether sulfone) s.* Journal of Power Sources, 2015. **279**: p. 48-54.
23. Zhu, Y., et al., *Enhanced chemical durability of perfluorosulfonic acid*

membranes through incorporation of terephthalic acid as radical scavenger. Journal of Membrane Science, 2013. **432**: p. 66-72.

24. Zhao, D., et al., *MnO 2/SiO 2–SO 3 H nanocomposite as hydrogen peroxide scavenger for durability improvement in proton exchange membranes.* Journal of Membrane Science, 2010. **346**(1): p. 143-151.
25. Buchmüller, Y., A. Wokaun, and L. Gubler, *Polymer-bound antioxidants in grafted membranes for fuel cells.* Journal of Materials Chemistry A, 2014. **2**(16): p. 5870-5882.
26. Wang, L., et al., *Preparation and properties of highly branched sulfonated poly (ether ether ketone) s doped with antioxidant 1010 as proton exchange membranes.* Journal of Membrane Science, 2011. **379**(1): p. 440-448.
27. Yao, Y., et al., *Vitamin E assisted polymer electrolyte fuel cells.* Energy & Environmental Science, 2014. **7**(10): p. 3362-3370.
28. Mikhailenko, S.D., F. Celso, and S. Kaliaguine, *Properties of SPEEK based membranes modified with a free radical scavenger.* Journal of Membrane Science, 2009. **345**(1): p. 315-322.
29. Kim, Y., et al., *A polyoxometalate coupled graphene oxide–Nafion composite membrane for fuel cells operating at low relative humidity.* Journal of Materials Chemistry A, 2015. **3**(15): p. 8148-8155.
30. Xue, C., et al., *Graphite oxide/functionalized graphene oxide and polybenzimidazole composite membranes for high temperature proton exchange membrane fuel cells.* International Journal of Hydrogen Energy, 2014. **39**(15): p. 7931-7939.
31. Lee, D., et al., *Nafion/graphene oxide composite membranes for low humidifying polymer electrolyte membrane fuel cell.* Journal of Membrane Science, 2014. **452**: p. 20-28.
32. Kumar, R., M. Mamlouk, and K. Scott, *Sulfonated polyether ether ketone–sulfonated graphene oxide composite membranes for polymer electrolyte fuel cells.* RSC Advances, 2014. **4**(2): p. 617-623.
33. Pandey, R.P. and V.K. Shahi, *Sulphonated imidized graphene oxide (SIGO) based polymer electrolyte membrane for improved water retention, stability and proton conductivity.* Journal of Power Sources, 2015. **299**: p. 104-113.

34. Ueda, M., et al., *Synthesis and characterization of aromatic poly (ether sulfone) s containing pendant sodium sulfonate groups.* Journal of Polymer Science Part A: Polymer Chemistry, 1993. **31**(4): p. 853-858.
35. Kim, K., et al., *Poly (arlyene ether sulfone) based semi-interpenetrating polymer network membranes containing cross-linked poly (vinyl phosphonic acid) chains for fuel cell applications at high temperature and low humidity conditions.* Journal of Power Sources, 2015. **293**: p. 539-547.
36. Hara, N., et al., *Rapid proton conduction through unfreezable and bound water in a wholly aromatic pore-filling electrolyte membrane*. The Journal of Physical Chemistry B, 2009. **113**(14): p. 4656-4663.
37. Hwang, S.-H., et al., *Poly (vinyl alcohol) reinforced and toughened with poly (dopamine)-treated graphene oxide, and its use for humidity sensing.* ACS nano, 2014. **8**(7): p. 6739-6747.
38. Cao, K., et al., *Enhanced water permeation through sodium alginate membranes by incorporating graphene oxides.* Journal of Membrane Science, 2014. **469**: p. 272-283.
39. Lim, M.-Y., et al., *Effect of antioxidant grafted graphene oxides on the mechanical and thermal properties of polyketone composites.* European Polymer Journal, 2015. **69**: p. 156-167.
40. Yang, J., et al., *Novel composite membranes of triazole modified graphene oxide and polybenzimidazole for high temperature polymer electrolyte membrane fuel cell applications.* RSC Advances, 2015. **5**(122): p. 101049-101054.
41. Ko, T., et al., *Sulfonated poly (arylene ether sulfone) composite membranes having poly (2, 5-benzimidazole)-grafted graphene oxide for fuel cell applications.* Journal of Materials Chemistry A, 2015. **3**(41): p. 20595-20606.
42. Ingold, K.U. and D.A. Pratt, *Advances in radical-trapping antioxidant chemistry in the 21st century: a kinetics and mechanisms perspective.* Chemical reviews, 2014. **114**(18): p. 9022-9046.
43. Mishra, A.K., et al., *Enhanced mechanical properties and proton conductivity of Nafion–SPEEK–GO composite membranes for fuel cell applications.* Journal of Membrane Science, 2014. **458**: p. 128-135.

44. Tseng, C.Y., et al., *Sulfonated polyimide proton exchange membranes with graphene oxide show improved proton conductivity, methanol crossover impedance, and mechanical properties.* Advanced Energy Materials, 2011. **1**(6): p. 1220-1224.
45. Jeon, J.H., et al., *Dry-type artificial muscles based on pendent sulfonated chitosan and functionalized graphene oxide for greatly enhanced ionic interactions and mechanical stiffness.* Advanced Functional Materials, 2013. **23**(48): p. 6007-6018.
46. Lim, M.-Y., et al., *Improved strength and toughness of polyketone composites using extremely small amount of polyamide 6 grafted graphene oxides.* Carbon, 2014. **77**: p. 366-378.
47. Jiang, Z., et al., *Composite membranes based on sulfonated poly (ether ether ketone) and SDBS-adsorbed graphene oxide for direct methanol fuel cells.* Journal of Materials Chemistry, 2012. **22**(47): p. 24862-24869.
48. Kumar, R., C. Xu, and K. Scott, *Graphite oxide/Nafion composite membranes for polymer electrolyte fuel cells.* RSC Advances, 2012. **2**(23): p. 8777-8782.
49. He, Y., et al., *Polydopamine-modified graphene oxide nanocomposite membrane for proton exchange membrane fuel cell under anhydrous conditions.* Journal of Materials Chemistry A, 2014. **2**(25): p. 9548-9558.

국문 요약

라디칼 스캐빈저의 기능을 갖는 HA-GO를 포함한 SPAES 복합막을 제조하였다. SPAES는 축합중합을 통해 합성하였으며, HA-GO는 그래핀 옥사이드의 에폭시와 HA의 아민의 고리 열림 반응을 통해 제조하였다. 복합막의 HA-GO 함량이 증가함에 따라 물리적 성질, 치수 안정성, 수소이온 전도도가 향상되었다. 특별히 항산화 기능을 갖는 HA-GO의 영향으로 복합막의 화학적 안정성이 증가하였다. 그리고 가장 좋은 성능을 보인 SPAES/HA-GO_0.5는 산화 안정성 실험 후 수소이온 전도도의 감소폭이 SPAES 단일막과 SPAES/GO_0.5 복합막 보다 줄어든 수치를 나타내었다. 이는 HA-GO가 우수한 산화 안정성을 나타내기 때문이다.

주요어: 힌더드 아민, 항산화물질, 술폰화 폴리(아릴렌 에테르 술폰), 그래핀 옥사이드, 고분자 전해질 막 연료전지

공학석사학위논문

연료전지 응용을 위한 항산화 기능을 갖는 그래핀 옥사이드가 도입된 폴리(아릴렌 에테르 술폰) 복합막의 합성과 분석

Synthesis and Characterization of Poly(arylene ether sulfone)/Functionalized Graphene Oxide Composite Membrane Having Antioxidant Property for Fuel Cell Applications

2016년 2월

서울대학교 대학원

화학생물공학부

배 중 문

Abstract

Synthesis and Characterization of Poly(arylene ether sulfone)/Functionalized Graphene Oxide Composite Membrane Having Antioxidant Property for Fuel Cell Applications

Jungmoon Bae

Polymer Chemistry

Department of Chemical & Biological Engineering

Seoul National University

Sulfonated poly(arylene ether sulfone) (SPAES) based composite membranes were prepared using hindered amine functionalized graphene oxide (HA-GO) as a hydroxyl radical scavenger to investigate the effect of functionalized GO filler on membrane properties such as chemical durability, mechanical properties, water absorption behavior, and proton conductivity. The SPAES was synthesized by nucleophilic addition, and the HA-GO was prepared by ring opening reaction between the amine unit in 4-Amino-2,2,6,6-tetramethylpiperidine and epoxy group in graphene oxide. When the HA-GO was incorporated into the SPAES

matrix, the mechanical strength, dimensional stability, and proton conductivity of the composite membranes were improved. Especially, the SPAES/HA-GO composite membranes revealed much enhanced chemical durability compared to the pristine SPAES membrane in Fenton's reagent at 70 ^{o}C due to antioxidant property of the hindered amine groups in HA-GO. Therefore, the SPAES/HA-GO composite membranes exhibited less destroyed surface structure, and lower proton conductivity decrease than the pristine SPAES membrane after immersing in Fenton's reagent at 90 ^{o}C.

Keywords: Hindered amine, Antioxidant, Sulfonated Poly(arylene ether sulfone) (SPAES), Graphene oxide (GO), Polymer electrolyte membrane fuel cell (PEMFC)

List of Tables

Table 1. Oxidative stability and mechanical properties of the membranes.

Table 2. IEC, water uptake, dimensional change of volume of the membranes, and proton conductivity at 90 ^{o}C, 50 % RH.

List of Figures

Figure 1. Synthesis of sulfonated poly(arylene ether sulfone) (SPAES).

Figure 2. ^{1}H-NMR spectra of SPAES.

Figure 3. Preparation of hindered amine graphene oxide (HA-GO).

Figure 4. FT-IR spectra of GO, HA-GO, and HA.

Figure 5. XPS spectra of HA-GO.

Figure 6. TGA curves of GO, and HA-GO under a N_2 atmosphere.

Figure 7. SEM images of the cross-section of the membranes. (a) SPAES, (b) SPAES/HA-GO_0.1, (c) SPAES/HA-GO_0.5, (d) SPAES/HA-GO_1.0, and (e) SPAES/HA-GO_3.0.

Figure 8. Oxidative stability of SPAES and SPAES/HA-GO composite membranes.

Figure 9. Proton conductivity of SPAES and SPAES/HA-GO composite membranes at 90 ^{o}C as a function of relative humidity.

Figure 10. Proton conductivity of SPAES, SPAES/HA-GO_0.5, and SPAES/GO_0.5 at 90 ^{o}C (a) before fenton test, and (b) after fenton test.

List of Contents

Abstract ---------- i

List of Tables----------iii

List of Figures----------iv

List of Contents----------vi

1. **Introduction**----------1

2. **Experimental**----------3

2.1. Materials----------3

2.2. Synthesis of sulfonated poly(arylene ether sulfone) (SPAES)----------4

2.3. Preparation of graphene oxide (GO) ----------5

2.4. Preparation of hindered amine grafted graphene oxide (HA-GO)----6

2.5. Preparation of composite membranes ----------7

2.6.Characterization----------7

3. Results and Discussion----------10

3.1. Synthesis of sulfonated poly(arylene ether sulfone) (SPAES)----------10

3.2. Characterization of functionalized graphene oxide----------15

3.3. Morphology of composite membranes----------21

3.4. Oxidative stability----------23

3.5. Mechanical properties----------27

3.6. IEC, water uptake, and dimensional change----------29

3.7. Proton conductivity----------32

4. Conclusion----------36

5. References----------37

6. Abstract in Korean----------42

1. Introduction

Subsequently to the industrial revolution, the conversion of chemical energy into electrical energy became more important due to the increase in the use of electricity. It leads to develop of variety technologies, and the polymer electrolyte membrane fuel cells (PEMFCs) is one of them.[1, 2] The PEMFCs are attractive as highly energy efficient and environmentally friendly alternative energy sources than other developing applications.[3, 4] The polymer electrolyte membrane (PEM), which is one of the most important components of PEMFCs, plays a vital role in conducting protons from the anode to the cathode and acts as a barrier. PEM should have a high proton conductivity, mechanical stability, and chemical stability for practical applications.[5]

The commercially available and most studied PEM materials are perfluorosulfonated ionomers, such as Nafion, due to their high proton conductivity value and good chemical stability.[6] But perfluorosulfonated ionomers have some limitations such as high cost, low operational temperature (< 80 ^{o}C), and high gas permeability. Therefore, many groups try to overcome these limitations by developing modified perfluorosulfonated ionomer derivatives and alternative materials such as aromatic hydrocarbon polymers. Several groups of

advanced aromatic hydrocarbon based polymers were synthesized to develop PEM materials such as sulfonated poly(arylene ether sulfone) (SPAES),[7-9] sulfonated poly(ether ether ketone) (SPEEK),[10, 11] sulfonated polyimide (SPI),[12] polybenzimidazole (PBI).[13-15] Those kind of aromatic hydrocarbon polymers have merits of low cost, high thermal stability, and low gas permeability. Among these alternatives, SPAES is a considerably attractive material because of its high stability under operation condition in fuel cell.[16]

Recently, durability of the PEM is one of the critical issues impending commercialization of PEMFCs.[17, 18] It has relevance to chemical degradation of membrane according to hydroxyl radicals. The chemical reaction on the catalyst in anode and cathode can produce hydroxyl radicals, which are widely known to be responsible for chemical attack on the membrane.[19, 20] In the sulfonated poly(arylene ether sulfone) case, two possible degradation mechanisms, detachment of the sulfonic groups and polymer chain scission, are believed.[21, 22] Detachment of the sulfonic groups in membrane will cause a lowering of proton conductivity and polymer chain scission will cause a cell lifetime issue. Several groups research membranes containing radical scavenger materials.[23-28] In addition, graphene oxide (GO) has been extensively used for polymer composites due to its large surface area, great mechanical strength, chemical stability, and functional groups. To enhance the physicochemical properties of GO

have recently been studied.[29-33]

In this study, hindered amine functionalized graphene oxide was prepared by ring opening reaction between graphene oxide and 4-Amino-2,2,6,6-tetramethylpiperidine for use as a filler to improve the chemical stability and mechanical strength of PEM. This study provides a description of the synthesis and properties of the composite membranes, including their oxidative stability, mechanical stability, water absorption properties, and proton conductivity.

2. Experimental

2.1.Materials

4,4’-Dihydroxybiphenyl (BP, 97.0%, Aldrich) was recrystallized from methanol. 4,4’-Dichlorodiphenylsulfone (DCDPS, 98.0%, Aldrich) was recrystallized from toluene and 3,3’-Disulfonate-4,4’-dichlorodiphenylsulfone (SDCDPS) was synthesized from DCDPS according to previous literature.[34] Graphite powders were received from BASF (Germany). 4-Amino-2,2,6,6-

tetramethylpiperidine (HA, 97.0%, TCI) was used as received. *N*-Methyl-2-pyrrolidone (NMP, 99.0%, Junsei) and *N*,*N*-Dimethylformamide (DMF, 99.5%, Junsei) were stored over molecular sieves. Potassium carbonate (K_2CO_3, 99.0%, Aldrich), Phosphorous pentoxide (P_2O_5, 99.99+%, Aldrich), Sodium nitrate ($NaNO_3$, 99.0%, Daejung), and Potassium permanganate ($KMnO_4$, 97.0%, Aldrich) were used as received. All other solvents and reagents were used as received from standard vendors.

2.2.Synthesis of sulfonated poly(arylene ether sulfone) (SPAES)

SPAES was synthesized by condensation reaction between the 4,4'-Dihydroxybiphenyl (BP) and the dichloro monomers such as 4,4'-Dichlorodiphenylsulfone (DCDPS), and 3,3'-Disulfonate-4,4'-dichlorodiphenylsulfone (SDCDPS). A 250 mL three-neck round bottom flask equipped with nitrogen inlet and outlet, Dean-Stark trap, condenser, and mechanical stirrer was charged with 5.00 g (26.9 mmol) of BP, 3.86 g (13.4 mmol)

of DCDPS, 6.60 g (13.4 mmol) of SDCDPS, and 4.27 g (30.9 mmol) of K_2CO_3 in 45.2 mL of NMP. Then 22.6 mL of toluene (NMP/toluene = 2/1, v/v) was added as an azeotroping agent. The mixture was heated 145 ^oC for 4 h. And the toluene was removed, the bath temperature was raised to 190 ^oC for polymerization. After 48 h, viscous solution was cooled down to room temperature and diluted with 10.0 mL of NMP. The solution was filtered and precipitated in *iso*-propylalcohol (1000mL) to remove the salt. And then, the white product obtained from precipitation was dried overnight under vacuum.

2.3.Preparation of graphene oxide (GO)

Graphene oxide (GO) was synthesized by the modified Hummer's method using graphite as starting materials. 1.0 g of graphite powder and 0.5 g of P_2O_5 were added to 6 mL of concentrated sulfuric acid (98.0%). The mixture was heated at 80 ^oC and stirred for 6 h. Next, 200 mL of deionized water was added to the mixture. Then the mixture was filtered and washed with deionized water several times. The obtained product (pre-oxidized graphite) was dried in vacuum

oven at 60 ^{o}C for 24 h. The dried pre-oxidized graphite and 0.5 g $NaNO_3$ were added to 23 mL of concentrated sulfuric acid (98.0%) in an ice bath for 30 min without stirring. Next, 6.0 g of $KMnO_4$ was added slowly with stirring. The mixture was heated to 35 ^{o}C and stirred for 18 h. Then 200 mL of deionized water and 10 mL of 30 % H_2O_2 were added. The mixture was washed rinsing and centrifugation with 10 wt.% of HCl and deionized water for several times. The obtained product (GO) was dried overnight at 60 ^{o}C.

2.4.Preparation of hindered amine grafted graphene oxide (HA-GO)

0.1 g of GO was added to 30 mL of anhydrous DMF and the mixture was sonicated for 30 min. 0.2 g of 4-Amino-2,2,6,6-tetramethylpiperidine (hindered amine compound, HA, 1.28 mmol) was added to the GO solution and the mixture was heated at 80 ^{o}C with stirring and purged under N_2 for 12 h. Purified HA-GO was obtained by filtering through PTFE membrane filter with 0.2 μm pore size and washing with DMF several times.

2.5.Preparation of composite membranes

Composite membranes were prepared by solution casting. 0.5 mg of HA-GO (HA-GO/SPAES = 0.1/1 wt./wt.) was added to 3.33 g of DMF. The solution was sonicated for 40 min, and stirred at 60 ^{o}C for 1 h to make a homogeneous dispersion. And then, 0.5 g of SPAES was added to the solution and stirred at 60 ^{o}C for 2 h. Next, the solution was spread onto a glass plate. Thickness of membrane was controlled by a doctor blade film applicator. The casted solution was heated at 80 ^{o}C for 12 h in a vacuum oven. The obtained film was peeled off from the glass plate with deionized water and soaked in H_2SO_4 for 24 h. And then, the film was washed with deionized water. The samples are assigned as SPAES/HA-GO_X, where X is the wt% of HA-GO (X = 0.1, 0.5, 1.0, 3.0). For comparison of the HA-GO and GO, SPAES/GO_X composite membranes were prepared by same method.

2.6.Characterization

The ^{1}H-NMR spectra was collected on Avance-400 (Bruker, Germany) with a proton frequency of 400 MHz. Deuterated dimethylsulfoxide (DMSO-d_6) and tetramethylsilane (TMS) were used as the solvent and the internal standard, respectively. M_n and M_w were measured by gel permeation chromatography (GPC) consisting of a Waters 510 HPLC pump at 35 ^{o}C, three columns PLgel 5 μm guard, MIXED-C, MIXED-D, and a Viscoter T60A dual detector. HPCL grade DMF was used as the eluent and the flow rate was 1.0 mL min^{-1}. Calibration was performed with polystyrene standards.

Fourier-transform infrared (FT-IR) spectra of samples were recorded on Nicolet 6700 (Thermo Scientific, USA) in the attenuated total reflectance (ATR) mode in the frequency range of 4000 to 650 cm^{-1}. The spectra were collected over 30 scans at 4 cm^{-1} resolution. Thermo gravimetric analysis (TGA) was performed in a Q-5000IR (TA instruments, USA). The samples were heated from 25 ^{o}C to 600 ^{o}C with a heating rate of 5 ^{o}C/min under nitrogen atmosphere. X-ray photoelectron spectroscopy (XPS) was carried out using MgKα (1254.0 eV) as the radiation source on a KRATOS AXIS-His. The spectra were collected over a range of 0-1200 eV. The cross-sectional morphology of the composite membranes was inspected by JSM-6700F (JEOL, Japan) using a field emission scanning electron microscope (FESEM).

The oxidative stability of the membranes was evaluated by Fenton's test. The membranes were soaked in Fenton's reagent (3% H_2O_2 containing 4 ppm Fe^{2+}) at 70^{o}C. The time when the membranes were degraded (τ_1) and dissolved (τ_2) was recorded. The mechanical properties were measured using a universal testing machine (UTM, Lloyd LR-10k, UK). And dumbbell specimens were prepared using the ASTM standard D638 (Type V specimens). The tensile properties of the samples were measured in air at 25 ^{o}C under a 40% relative humidity (RH) with a gauge length and cross head speed of 15 mm and 5 mm min^{-1}, respectively. At least 10 samples were tested for each sample.

Ion-exchange capacity (IEC) of the membranes was measured by back-titration method. The dry membranes were soaked in 1 M NaCl aqueous solution at 25 ^{o}C for 24 h. And the solution was titrated with 0.01 M NaOH aqueous solution. The value of IEC was calculated from the titration data as follows:

$$IEC\ [mequiv.g^{-1}] = (C_{NaOH} \cdot \triangle V_{NaOH} / W_s)\ X\ 1000$$

where C_{NaOH}, $\triangle V_{NaOH}$, and W_s are the concentration of NaOH (aq), the consumed volume of NaOH (aq), and the weight of the dry membrane, respectively. The water uptake and dimensional change of the membranes were determined by measuring their change in weight and volume. The dry membranes were cut into 1 cm X 5 cm, and then their weight and volumes were measured.

Thereafter, the membranes were put into deionized water at 30 ^{o}C and 90 ^{o}C for 24 h and 4 h, respectively. After the membranes were taken out and wiped, their weight and volumes were measured. The water uptake and dimensional change were calculated as follows:

Water uptake (%) = $[(W_{wet} - W_{dry})/W_{dry}] \times 100$

Dimensional change (%) = $[(V_{wey} - V_{dry})/V_{dry}] \times 100$

where W_{wet} and W_{dry} are the weight of the wet and dry membranes and V_{wet} and V_{dry} are the volume of the wet and dry membranes, respectively.

Proton conductivities of the composite membranes were measured using a conductivity measurement system (BekkTeck BT-552MX, USA) with a H_2 flow rate of 500 cm^3/min at 90^{o}C under different relative humidity (RH) conditions. The samples were pre-equilibrated at 90^{o}C and 70% RH for 2h, after that the conductivity of membrane was measured. The equilibrium RH was obtained after about 15 min of stabilization time.

3. Result and Discussion

3.1.Synthesis of sulfonated poly(arylene ether sulfone) (SPAES)

Sulfonated poly(arylene ether sulfone) was synthesized by nucleophilic addition between the 4,4'-Dihydroxybiphenyl (BP) and the dichloro monomers such as 4,4'-Dichlorodiphenylsulfone (DCDPS) and 3,3'-Disulfonate-4,4'-dichlorodiphenylsulfone (SDCDPS) in NMP which contained toluene as an azotropic agent (Fig. 1).[35] The chemical structure of SPAES was confirmed by ^{1}H-NMR spectroscopy (Fig. 2). Degree of sulfonation (DS) of polymer is important parameter affecting physical stability and proton conductivity of PEM. With increments of DS, the proton conductivity value of membrane increases because the membrane becomes more hydrophilic and absorbs more water, which facilitates proton transport. However, when the DS is above 50 %, the physical stability of membrane is not suitable for use fuel cell applications. Thus, we prepared SPAES with the DS of 50 % for the PEMFC test in our experiments. The DS of SPAES was calculated from the integral ratio of proton peaks in aromatic regions by following equation[36]

$$DS\ (\%) = [8 \cdot I_7 / (2 \cdot I_7 + I_{others})]\ X\ 100$$

where I_7 and I_{others} are the integral value of 7 proton signal and the sum of the integral value of other proton signals, respectively. According to Fig. 2, the DS of SPAES is 46 % although the feed molar ratio of SDCDPS and DCDPS is 1:1. Slightly different reactivity between SDCDPS and DCDPS is causing this

result.[35] The number average molecular weight (M_n) and weight average molecular weight (M_w) of the SPAES measured from the GPC were 36000 and 123000, respectively. We confirmed successful synthesis of SPAES with high molecular weight.

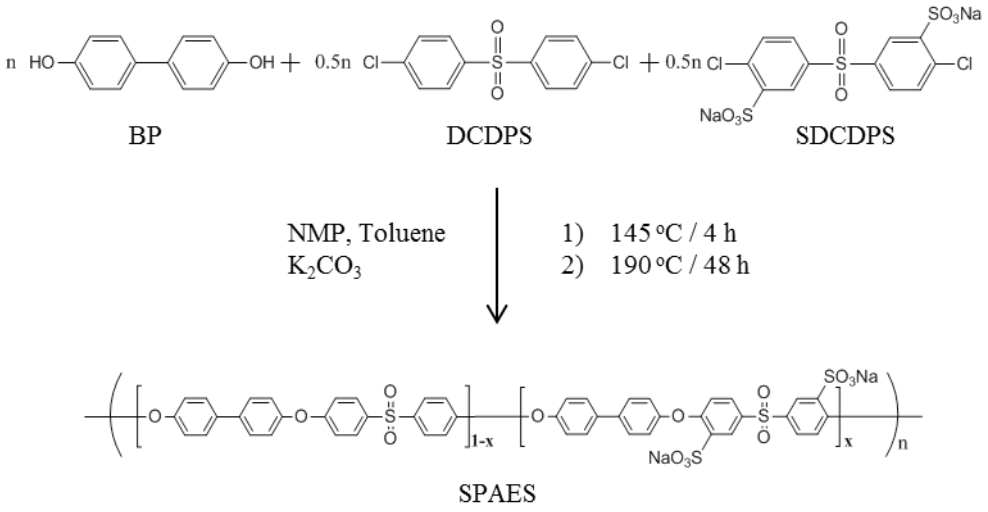

Figure 1. Synthesis of sulfonated poly(arylene ether sulfone) (SPAES).

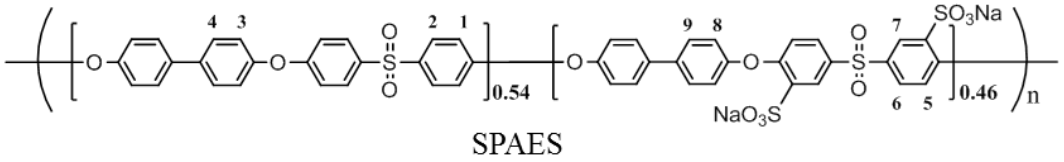

SPAES

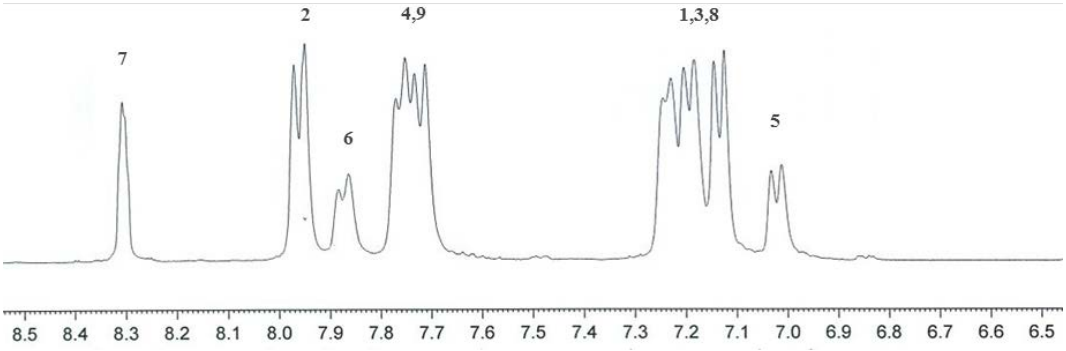

Figure 2. ^{1}H-NMR spectra of SPAES.

3.2.Characterization of functionalized graphene oxide

Graphene oxide (GO), and hindered amine functionalized graphene oxide (HA-GO) were prepared as shown in Fig. 3. GO was prepared from graphite by the modified Hummer's method with 6 weight equivalent amount of $KMnO_4$. HA-GO was prepared by ring opening reaction between the amine unit in hindered amine and epoxy group in GO. The chemical structure of GO and HA-GO was confirmed by FT-IR spectroscopy (Fig. 4). In the spectrum of GO, broad O-H stretching vibrations peak at 3450 cm^{-1}, C-O stretching vibrations peak at 1043 cm^{-1}, C=O stretching vibrations peak from carboxyl groups at 1740 cm^{-1}, and C-O-C stretching vibrations peak at 1248 cm^{-1} were observed.[37, 38] For HA-GO, peak of piperidine ring from the hindered amine at 2900-3000 cm^{-1}, and C-N stretching vibrations peak at 1440 cm^{-1} were observed. Also XPS results of HA-GO shown in the Fig. 5. The N 1_S peak was observed from the HA-GO.

The content of the grafted hindered amine on the GO were estimated by TGA (Fig. 6). The weight change below 300 °C of GO and HA-GO exhibits the thermal decomposition of the oxygen functional groups such as hydroxyl, epoxide, carboxylic acid, and ketone. And 14 wt% of the weight change of the HA-GO between 300 and 500 °C exhibits the thermal decomposition of the hindered

amine on the GO.[39] This results indicate the successful incorporation of the hindered amine unit into GO to from HA-GO.

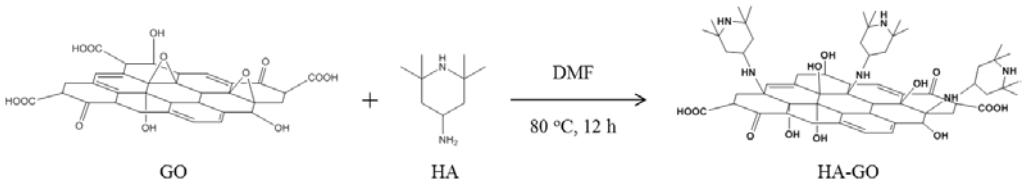

Figure 3. Preparation of hindered amine graphene oxide (HA-GO).

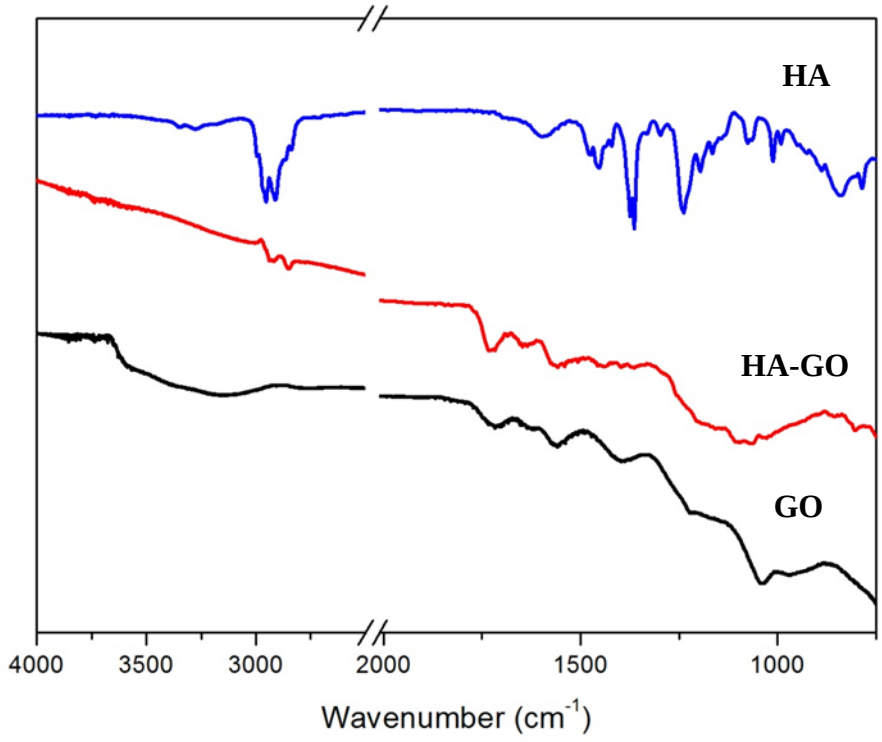

Figure 4. FT-IR spectra of GO, HA-GO, and HA.

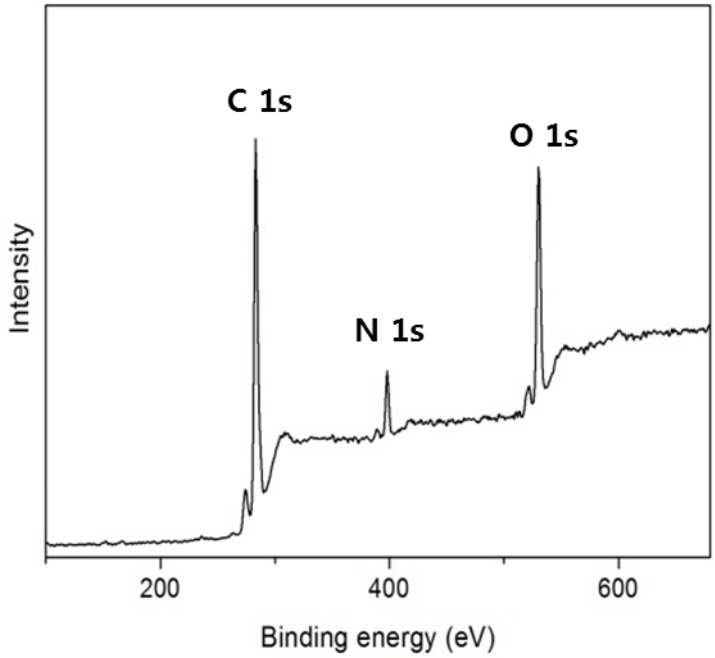

Figure 5. XPS spectra of HA-GO

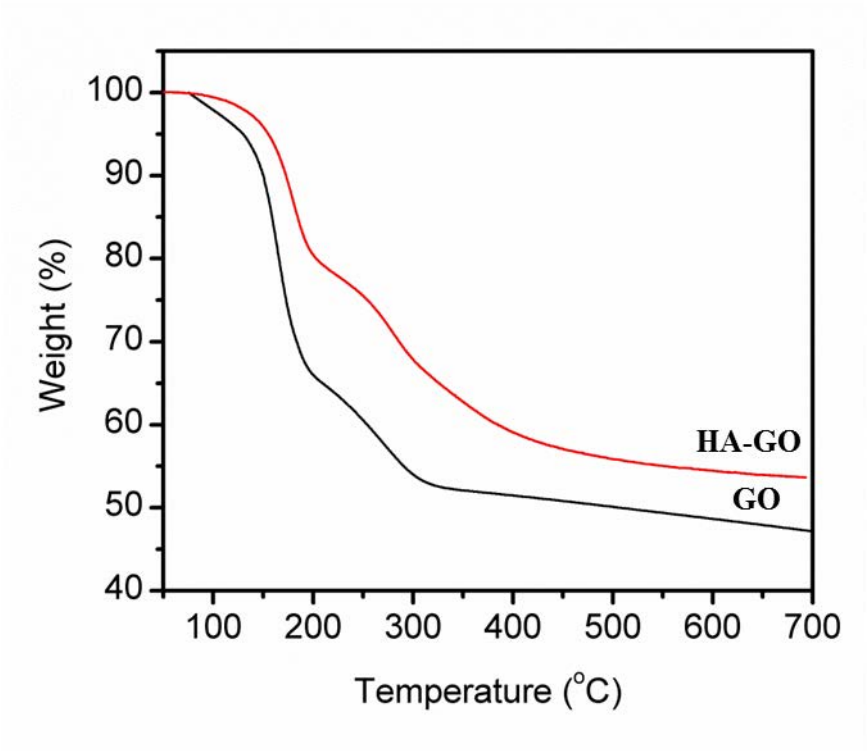

Figure 6. TGA curves of GO, and HA-GO under a N_2 atmosphere.

3.3.Morphology of composite membranes

The SPAES/HA-GO composite membranes were prepared successfully by solution casting method. Each thickness of the membranes was 15 ~ 20 μm. Internal morphology of the membranes showing filler dispersion was observed by cross-sectional SEM in Fig. 7. The cross-section of composite membranes was obtained by brittle breakage in liquid nitrogen. The pristine SPAES membrane showed relatively uniform and smooth cross-sectional features. But, when the HA-GO content increases, the morphology of the membranes became rougher due to the mutual interaction between the SPAES and HA-GO fillers. This result is because the GO generally has a poor dispersion in common organic solvent.[40] Especially, when HA-GO content is larger than 0.5 wt% in SPAES matrix, agglomerated domains form due to the poor dispersion of the HA-GO fillers. These agglomerated domains have a bad effect on drives of PEMFCs.[41]

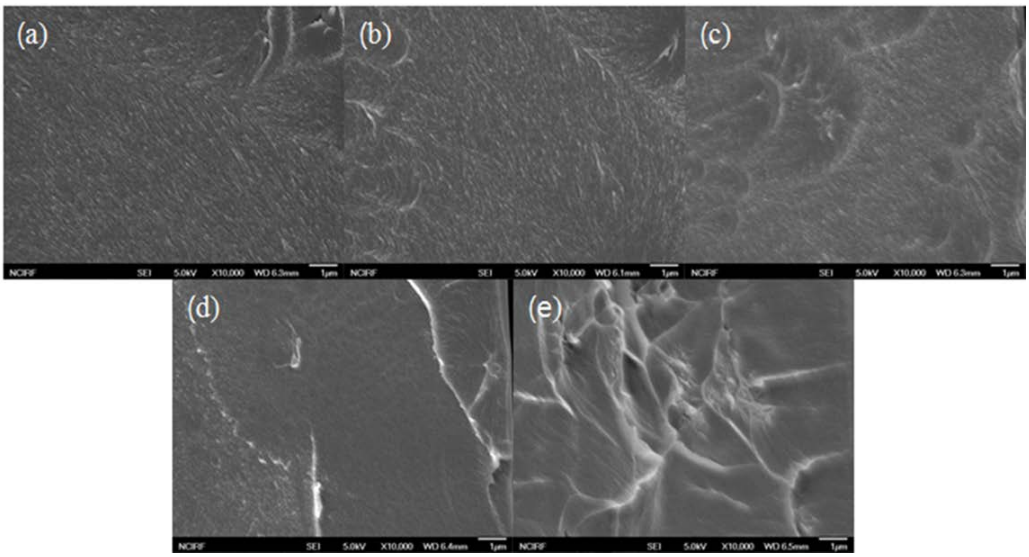

Figure 7. SEM images of the cross-section of the membranes. (a) SPAES, (b) SPAES/HA-GO_0.1, (c) SPAES/HA-GO_0.5, (d) SPAES/HA-GO_1.0, and (e) SPAES/HA-GO_3.0.

3.4.Oxidative stability

Oxidative stability is key parameter for durable PEM operation. The oxidative stability of SPAES/HA-GO composite membranes was investigated by Fenton test to evaluate the chemical stability of membranes against the attack of hydroxyl radical. The elapsed time was measured when the membranes start to break into pieces (τ_1), and the membranes are dissolved completely (τ_2) after immersion into Fenton's reagent (3 % H_2O_2 containing 4 ppm Fe^{2+}) at 70 ^oC. As shown in Fig. 8 and Table 1, the τ_1 and τ_2 value of the SPAES/HA-GO_0.5 were 480 min and 560 min, that of pristine SPAES were 387 min and 492 min, respectively. The oxidative stability increased by 24 % in τ_1 and 14 % in τ_2. It is observed that the incorporation of HA-GO into the SPAES matrix improved the oxidative stability of composite membranes compared to that of pristine SPAES when the content of the HA-GO contain below 0.5 wt% because HA works as a hydroxyl radical scavenger.[42] However, when the content of the HA-GO contain above 0.5 wt%, τ_1 and τ_2 value of composite membranes decreased. Because the aggregation of

HA-GO in the SPAES matrix when HA-GO contain above 0.5 wt% act the weak point that it is attacked by hydroxyl radicals.[43] Therefore, the addition of 0.5 wt% of HA-GO represents the most effective content to improve the oxidative stability of the PEM.

Table 1. Oxidative stability and mechanical properties of the membranes.

Samples	Fenton test		Tensile strength (MPa)	Elongation at break (%)
	τ_1 (min)	τ_2 (min)		
SPAES	387	492	62.9	10.3
SPAES/HA-GO_0.1	475	540	63.6	9.4
SPAES/HA-GO_0.5	480	560	65.3	6.5
SPAES/HA-GO_1.0	387	480	72.4	6.4
SPAES/HA-GO_3.0	340	450	73.4	6.2

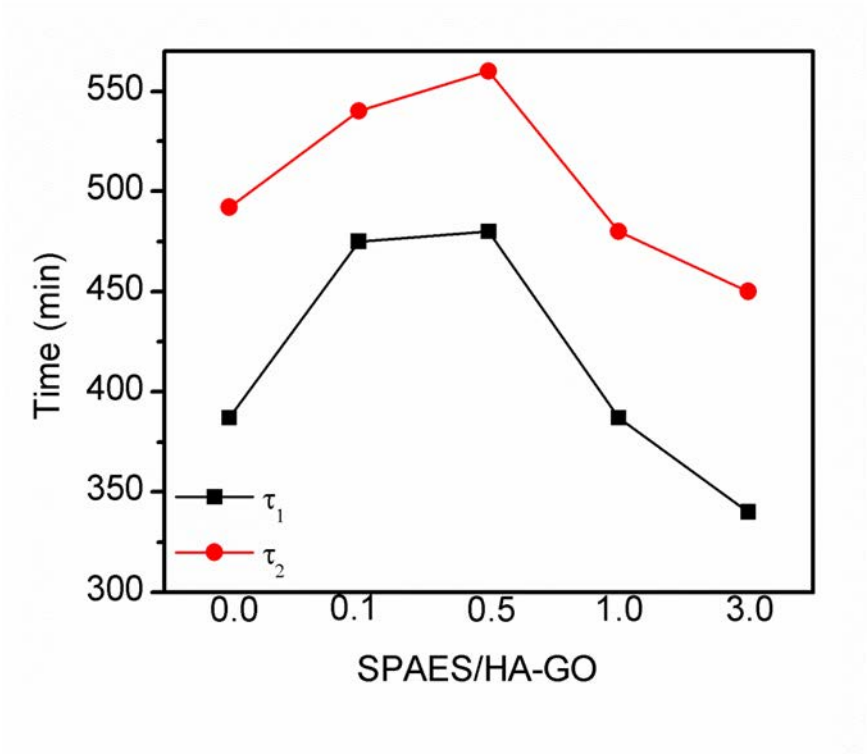

Figure 8. Oxidative stability of SPAES and SPAES/HA-GO composite membranes.

3.5.Mechanical properties

Adequate mechanical properties are essential for PEM for the fabrication of the membrane electrode assembly (MEA). The mechanical properties of membranes, such as tensile strength and elongation at break were measured by UTM under room temperature and 45 % RH conditions and shown in Table 1. The tensile strength of SPAES/HA-GO composite membranes was larger than pristine SPAES membrane and increased with increasing HA-GO content. On the contrary, elongation at break of SPAES/HA-GO composite membranes was smaller than pristine SPAES membrane and decreased with increasing HA-GO content. The SPAES/HA-GO_3.0 membrane had tensile strength of 74 MPa, and elongation at break of 6.1 %, that of pristine SPAES had tensile strength of 66 MPa, and elongation at break of 10.2 %. The tensile strength increased by 12 % and the elongation at break decreased by 40 % with the addition of HA-GO. Generally, the corporation of fillers, such as graphene and graphene oxide, in a polymer matrix enhances the mechanical strength by the reinforcement effect of the fillers.[44-46] Obviously, composite membranes increase the tensile strength and

decrease the elongation at break because HA-GO work as an effective filler in this study. This result demonstrated that the HA-GO as a filler in the polymer matrix was an effective approach for PEM with good mechanical properties.

3.6.IEC, water uptake, and dimensional change

IEC (the amount of exchangeable protons in membrane), water uptake, and dimensional change are important parameter affecting the quality of the PEM. In generally, PEM is required to have higher IEC and water uptake, but lower dimensional change, which would improve the performance of PEMFCs. The value of each parameter is shown Table 2. The IEC measured by a titration method. The IEC values decrease from 1.87 mequiv g^{-1} to 1.75 mequiv. g^{-1} when HA-GO contents increased.

The water uptake and dimensional change are the important factors which affect proton conductivity and mechanical properties of PEM. A suitable amount of water in membrane can forward proton transport, but excessive water absorption lead to side effects such as deterioration of mechanical strength.[41] Therefore, suitable water absorption is required for the PEMFCs. In this study, while functionalized graphene oxide formed free volume in polymer matrix to absorb water, strong interaction between functionalized graphene oxide and SPAES enhanced maintained dimensions. As expected, the water uptake increased with increasing the HA-GO content. The water uptake of SPAES/HA-GO_3.0 was 79.2 % at 30 ^{o}C and 121.5 % at 90 ^{o}C, and the water uptake of pristine SPAES

was 67.7 % at 30 ^{o}C and 93.1 % at 90 ^{o}C. The water uptake increased with increasing HA-GO content due to the hydrophilic nature of GO, and increasing free volume of polymer matrix.[43] The dimensional change of composite membranes decreased with increasing the HA-GO content. The dimensional change of SPAES/HA-GO_3.0 was 21.5 % at 30 ^{o}C and 29.9 % at 90 ^{o}C, and the dimensional change of pristine SPAES was 69.2 % at 30 ^{o}C and 101.3 % at 90 ^{o}C. The SPAES /HA-GO composite membranes exhibited smaller dimensional change value than pristine SPAES membrane due to the acid-base interaction between the amine groups of HA-GO and sulfonic acid groups of the SPAES.[41] The large water uptake and smaller dimensional change values of SPAES/HA-GO composite membranes can be beneficial for PEMFCs because it can increase proton conductivity and mechanical stability.

Table 2. IEC, water uptake, dimensional change of volume of the membranes, and proton conductivity at 90 ^{o}C, 50 % RH.

Samples	IEC (mequiv g^{-1})	Water uptake (%)		Dimensional change of volume (%)		Proton conductivity (mS cm^{-1})
		30 °C	90 °C	30 °C	90 °C	
SPAES	1.87	67.7	93.1	69.2	101.3	9.7
SPAES/HA-GO_0.1	1.83	71.3	106.6	33.9	64.3	12.1
SPAES/HA-GO_0.5	1.81	75.9	111.3	33.1	56.7	17.0
SPAES/HA-GO_1.0	1.77	78.4	119.6	28.3	45.2	15.0
SPAES/HA-GO_3.0	1.75	79.2	121.5	21.5	29.9	15.0

3.7.Proton conductivity

The proton conductivity is critical property of the PEM, since high proton conductivity is necessary for their effective utilization in PEMFCs. Fig. 9 and Table 2 show the humidity dependence of the proton conductivity for all membranes at 90 ^{o}C. The proton conductivity of SPAES and composite membranes is sensitive to humidity and rises with the increase in relative humidity (RH) from 20 to 100 %. And up to 0.5 wt% of HA-GO, the proton conductivity increased, but beyond 0.5 wt%, the proton conductivity decreased. The proton conductivity of SPAES/HA-GO_0.5 was 1.70 x 10^{-2} S cm^{-1}, that of pristine SPAES was 0.97 x 10^{-2} S cm^{-1} at 50 %RH. It increased by 75 % with the addition of HA-GO. This result is because the increase in hydrophilic moieties from the HA-GO which results in more hydrophilic channels in which protons can pass through. However, beyond 0.5 wt% of HA-GO show a reduction in proton conductivity values because aggregated HA-GO works as a barrier that disconnects the hydrophilic channels.

In addition, after fenton test (3% H_2O_2 containing 4 ppm Fe^{2+}) at 90 ^{o}C for 1 h, proton conductivity of membranes was measured for chemical durability of PEM at 90 ^{o}C. As shown in Fig. 10, the pristine SPAES membrane, the SPAES/HA-GO_0.5 exhibited best performance such as oxidative stability and proton

conductivity, and SPAES/GO_0.5 as control group were measured. Before fenton test, proton conductivity of the pristine SPAES, SPAES/HA-GO_0.5, SPAES/GO_0.5 were 0.97 x 10^{-2} S cm^{-1}, 1.70 x 10^{-2} S cm^{-1}, and 1.71 x 10^{-2} S cm^{-1}, respectively. Recent studies were reported that the proton conductivity of PEM increased when the GO was incorporated into polymer matrix.[47-49] The SPAES/GO_0.5 exhibited higher proton conductivity value than pristine SPAES membrane due to the increase in hydrophilic moieties from the GO. After fenton test, proton conductivity of the pristine SPAES, SPAES/HA-GO_0.5, and SPAES/GO_0.5 were 0.58 x 10^{-2} S cm^{-1}, 1.30 x 10^{-2} S cm^{-1}, and 1.16 x 10^{-2} S cm^{-1}, respectively. And decrease of the proton conductivity of the membranes was 40.2 %, 23.5%, and 32.2 %, respectively. Decrease of the proton conductivity of the SPAES/GO_0.5 is smaller than pristine SPAES because GO has antioxidant property. The SPAES/HA-GO_0.5 was exhibited the best performance in this test. This result is because the HA molecules on the GO would rapidly trap the hydroxyl radicals and stop their attacks to the polymer chain, thus giving much higher proton conductivity than pristine SPAES.[42]

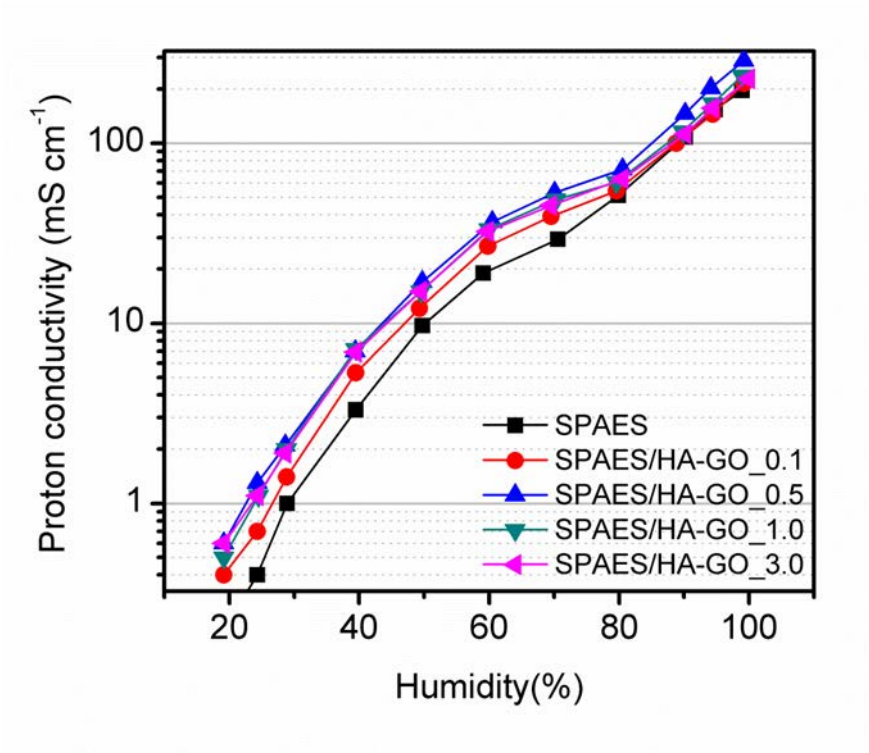

Figure 9. Proton conductivity of SPAES and SPAES/HA-GO composite membranes at 90 ^{o}C as a function of relative humidity.

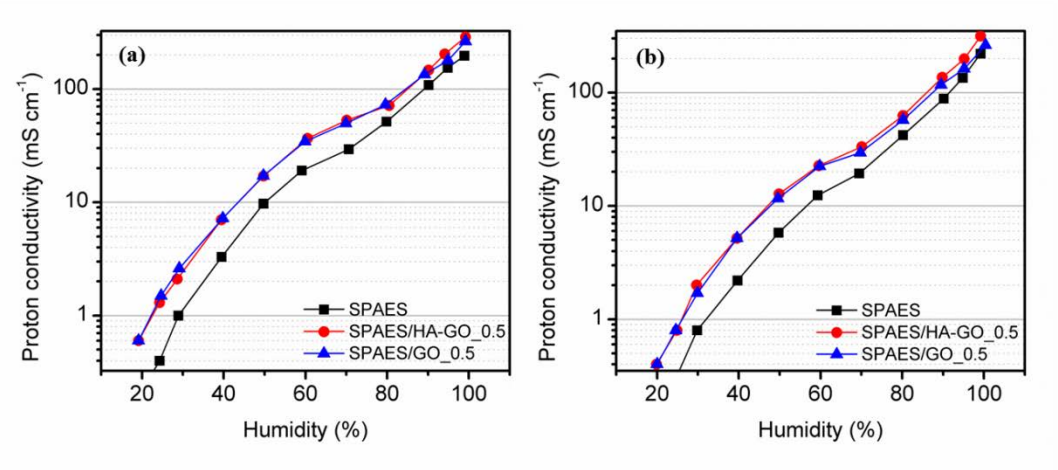

Figure 10. Proton conductivity of SPAES, SPAES/HA-GO_0.5, and SPAES/GO_0.5 at 90 ^{o}C (a) before fenton test, and (b) after fenton test.

4. Conclusion

Sulfonated poly(arylene ether sulfone) (SPAES) composite membranes were prepared using hindered amine (HA) grafted graphene oxide (HA-GO) for efficient polymer electrolyte membranes fuel cells (PEMFCs). The composite membranes showed improved mechanical properties and dimensional change due to an effective filler of HA-GO and acid-base interaction between SPAES and HA-GO. Especially, antioxidant property of the hindered amine should increase the oxidative stability of the membrane. SPAES/HA-GO_0.5 has shown better proton conductivity in comparison to pristine SPAES. Also, after fenton test at 90 ^{o}C for 1 h, decrease of the proton conductivity of the SPAES/HA-GO_0.5 was smaller than other membranes because HA-GO has antioxidant property. Therefore, we believe that the incorporation of HA-GO as a filler can be promising to develop proton exchange membranes for fuel cell applications.

5. References

1. Steele, B.C. and A. Heinzel, *Materials for fuel-cell technologies.* Nature, 2001. **414**(6861): p. 345-352.
2. Carrette, L., K. Friedrich, and U. Stimming, *Fuel cells–fundamentals and applications.* Fuel cells, 2001. **1**(1): p. 5-39.
3. Shao, Y., et al., *Proton exchange membrane fuel cell from low temperature to high temperature: material challenges.* Journal of Power Sources, 2007. **167**(2): p. 235-242.
4. Kim, S.-K., et al., *Durable cross-linked copolymer membranes based on poly (benzoxazine) and poly (2, 5-benzimidazole) for use in fuel cells at elevated temperatures.* Journal of Materials Chemistry, 2012. **22**(15): p. 7194-7205.
5. Hickner, M.A., et al., *Alternative polymer systems for proton exchange membranes (PEMs).* Chemical reviews, 2004. **104**(10): p. 4587-4612.
6. Paik, Y., S.S. Kim, and O.H. Han, *Methanol behavior in direct methanol fuel cells.* Angewandte Chemie International Edition, 2008. **47**(1): p. 94-96.
7. Kim, K., et al., *Semi-interpenetrating network electrolyte membranes based on sulfonated poly (arylene ether sulfone) for fuel cells at high temperature and low humidity conditions.* Electrochemistry Communications, 2014. **48**: p. 44-48.
8. Ko, T., et al., *Cross-Linked Sulfonated Poly (arylene ether sulfone) Membranes Formed by in Situ Casting and Click Reaction for Applications in Fuel Cells.* Macromolecules, 2015. **48**(4): p. 1104-1114.
9. Li, N., et al., *Enhancement of proton transport by nanochannels in comb-shaped copoly (arylene ether sulfone) s.* Angewandte Chemie, 2011. **123**(39): p. 9324-9327.
10. Xing, P., et al., *Synthesis and characterization of sulfonated poly (ether ether ketone) for proton exchange membranes.* Journal of Membrane Science, 2004. **229**(1): p. 95-106.
11. Zhao, C., et al., *High-performance proton exchange membranes for direct methanol fuel cells based on a SPEEK/polybenzoxazine crosslinked structure.* RSC Advances, 2015. **5**(59): p. 47284-47293.
12. Woo, Y., et al., *Synthesis and characterization of sulfonated polyimide*

membranes for direct methanol fuel cell. Journal of Membrane Science, 2003. **220**(1): p. 31-45.

13. Kim, S.-K., et al., *Highly durable polymer electrolyte membranes at elevated temperature: Cross-linked copolymer structure consisting of poly (benzoxazine) and poly (benzimidazole).* Journal of Power Sources, 2013. **226**: p. 346-353.
14. Kim, T.-H., T.-W. Lim, and J.-C. Lee, *High-temperature fuel cell membranes based on mechanically stable para-ordered polybenzimidazole prepared by direct casting.* Journal of Power Sources, 2007. **172**(1): p. 172-179.
15. Kim, S.-K., et al., *Cross-linked benzoxazine–benzimidazole copolymer electrolyte membranes for fuel cells at elevated temperature.* Macromolecules, 2012. **45**(3): p. 1438-1446.
16. Wang, F., et al., *Direct polymerization of sulfonated poly (arylene ether sulfone) random (statistical) copolymers: candidates for new proton exchange membranes.* Journal of Membrane Science, 2002. **197**(1): p. 231-242.
17. Zhao, D., et al., *A Durable Alternative for Proton-Exchange Membranes: Sulfonated Poly (Benzoxazole Thioether Sulfone) s.* Advanced Energy Materials, 2011. **1**(2): p. 203-211.
18. Alsheheri, J.M., H. Ghassemi, and D.A. Schiraldi, *Chemical degradation of fluorosulfonamide fuel cell membrane polymer model compounds.* Journal of Power Sources, 2014. **267**: p. 316-322.
19. Wu, J., et al., *A review of PEM fuel cell durability: degradation mechanisms and mitigation strategies.* Journal of Power Sources, 2008. **184**(1): p. 104-119.
20. Rodgers, M.P., et al., *Fuel cell perfluorinated sulfonic acid membrane degradation correlating accelerated stress testing and lifetime.* Chemical reviews, 2012. **112**(11): p. 6075-6103.
21. Lawrence, J. and T. Yamaguchi, *The degradation mechanism of sulfonated poly (arylene ether sulfone) s in an oxidative environment.* Journal of Membrane Science, 2008. **325**(2): p. 633-640.
22. Lawrence, J., K. Yamashita, and T. Yamaguchi, *Correlating electronic structure and chemical durability of sulfonated poly (arylene ether sulfone) s.* Journal of Power Sources, 2015. **279**: p. 48-54.
23. Zhu, Y., et al., *Enhanced chemical durability of perfluorosulfonic acid*

membranes through incorporation of terephthalic acid as radical scavenger. Journal of Membrane Science, 2013. **432**: p. 66-72.

24. Zhao, D., et al., *MnO 2/SiO 2–SO 3 H nanocomposite as hydrogen peroxide scavenger for durability improvement in proton exchange membranes.* Journal of Membrane Science, 2010. **346**(1): p. 143-151.
25. Buchmüller, Y., A. Wokaun, and L. Gubler, *Polymer-bound antioxidants in grafted membranes for fuel cells.* Journal of Materials Chemistry A, 2014. **2**(16): p. 5870-5882.
26. Wang, L., et al., *Preparation and properties of highly branched sulfonated poly (ether ether ketone) s doped with antioxidant 1010 as proton exchange membranes.* Journal of Membrane Science, 2011. **379**(1): p. 440-448.
27. Yao, Y., et al., *Vitamin E assisted polymer electrolyte fuel cells.* Energy & Environmental Science, 2014. **7**(10): p. 3362-3370.
28. Mikhailenko, S.D., F. Celso, and S. Kaliaguine, *Properties of SPEEK based membranes modified with a free radical scavenger.* Journal of Membrane Science, 2009. **345**(1): p. 315-322.
29. Kim, Y., et al., *A polyoxometalate coupled graphene oxide–Nafion composite membrane for fuel cells operating at low relative humidity.* Journal of Materials Chemistry A, 2015. **3**(15): p. 8148-8155.
30. Xue, C., et al., *Graphite oxide/functionalized graphene oxide and polybenzimidazole composite membranes for high temperature proton exchange membrane fuel cells.* International Journal of Hydrogen Energy, 2014. **39**(15): p. 7931-7939.
31. Lee, D., et al., *Nafion/graphene oxide composite membranes for low humidifying polymer electrolyte membrane fuel cell.* Journal of Membrane Science, 2014. **452**: p. 20-28.
32. Kumar, R., M. Mamlouk, and K. Scott, *Sulfonated polyether ether ketone–sulfonated graphene oxide composite membranes for polymer electrolyte fuel cells.* RSC Advances, 2014. **4**(2): p. 617-623.
33. Pandey, R.P. and V.K. Shahi, *Sulphonated imidized graphene oxide (SIGO) based polymer electrolyte membrane for improved water retention, stability and proton conductivity.* Journal of Power Sources, 2015. **299**: p. 104-113.

34. Ueda, M., et al., *Synthesis and characterization of aromatic poly (ether sulfone) s containing pendant sodium sulfonate groups.* Journal of Polymer Science Part A: Polymer Chemistry, 1993. **31**(4): p. 853-858.
35. Kim, K., et al., *Poly (arlyene ether sulfone) based semi-interpenetrating polymer network membranes containing cross-linked poly (vinyl phosphonic acid) chains for fuel cell applications at high temperature and low humidity conditions.* Journal of Power Sources, 2015. **293**: p. 539-547.
36. Hara, N., et al., *Rapid proton conduction through unfreezable and bound water in a wholly aromatic pore-filling electrolyte membrane*. The Journal of Physical Chemistry B, 2009. **113**(14): p. 4656-4663.
37. Hwang, S.-H., et al., *Poly (vinyl alcohol) reinforced and toughened with poly (dopamine)-treated graphene oxide, and its use for humidity sensing.* ACS nano, 2014. **8**(7): p. 6739-6747.
38. Cao, K., et al., *Enhanced water permeation through sodium alginate membranes by incorporating graphene oxides.* Journal of Membrane Science, 2014. **469**: p. 272-283.
39. Lim, M.-Y., et al., *Effect of antioxidant grafted graphene oxides on the mechanical and thermal properties of polyketone composites.* European Polymer Journal, 2015. **69**: p. 156-167.
40. Yang, J., et al., *Novel composite membranes of triazole modified graphene oxide and polybenzimidazole for high temperature polymer electrolyte membrane fuel cell applications.* RSC Advances, 2015. **5**(122): p. 101049-101054.
41. Ko, T., et al., *Sulfonated poly (arylene ether sulfone) composite membranes having poly (2, 5-benzimidazole)-grafted graphene oxide for fuel cell applications.* Journal of Materials Chemistry A, 2015. **3**(41): p. 20595-20606.
42. Ingold, K.U. and D.A. Pratt, *Advances in radical-trapping antioxidant chemistry in the 21st century: a kinetics and mechanisms perspective.* Chemical reviews, 2014. **114**(18): p. 9022-9046.
43. Mishra, A.K., et al., *Enhanced mechanical properties and proton conductivity of Nafion–SPEEK–GO composite membranes for fuel cell applications.* Journal of Membrane Science, 2014. **458**: p. 128-135.

44. Tseng, C.Y., et al., *Sulfonated polyimide proton exchange membranes with graphene oxide show improved proton conductivity, methanol crossover impedance, and mechanical properties.* Advanced Energy Materials, 2011. **1**(6): p. 1220-1224.
45. Jeon, J.H., et al., *Dry-type artificial muscles based on pendent sulfonated chitosan and functionalized graphene oxide for greatly enhanced ionic interactions and mechanical stiffness.* Advanced Functional Materials, 2013. **23**(48): p. 6007-6018.
46. Lim, M.-Y., et al., *Improved strength and toughness of polyketone composites using extremely small amount of polyamide 6 grafted graphene oxides.* Carbon, 2014. **77**: p. 366-378.
47. Jiang, Z., et al., *Composite membranes based on sulfonated poly (ether ether ketone) and SDBS-adsorbed graphene oxide for direct methanol fuel cells.* Journal of Materials Chemistry, 2012. **22**(47): p. 24862-24869.
48. Kumar, R., C. Xu, and K. Scott, *Graphite oxide/Nafion composite membranes for polymer electrolyte fuel cells.* RSC Advances, 2012. **2**(23): p. 8777-8782.
49. He, Y., et al., *Polydopamine-modified graphene oxide nanocomposite membrane for proton exchange membrane fuel cell under anhydrous conditions.* Journal of Materials Chemistry A, 2014. **2**(25): p. 9548-9558.

국문 요약

라디칼 스캐빈저의 기능을 갖는 HA-GO를 포함한 SPAES 복합막을 제조하였다. SPAES는 축합중합을 통해 합성하였으며, HA-GO는 그래핀 옥사이드의 에폭시와 HA의 아민의 고리 열림 반응을 통해 제조하였다. 복합막의 HA-GO 함량이 증가함에 따라 물리적 성질, 치수 안정성, 수소이온 전도도가 향상되었다. 특별히 항산화 기능을 갖는 HA-GO의 영향으로 복합막의 화학적 안정성이 증가하였다. 그리고 가장 좋은 성능을 보인 SPAES/HA-GO_0.5는 산화 안정성 실험 후 수소이온 전도도의 감소폭이 SPAES 단일막과 SPAES/GO_0.5 복합막 보다 줄어든 수치를 나타내었다. 이는 HA-GO가 우수한 산화 안정성을 나타내기 때문이다.

주요어: 힌더드 아민, 항산화물질, 술폰화 폴리(아릴렌 에테르 술폰), 그래핀 옥사이드, 고분자 전해질 막 연료전지